Contract Design in Renewable Energy Auctions: Evidence from India

Anshuman Bhakri[*]

October 30, 2024

Abstract

In procurement auctions, contracts set the post-auction investment terms. Under future uncertainty, incomplete contracts result in under-investment. This paper proposes contract design for the Indian solar energy procurement auctions to help achieve their green energy targets at the lowest possible procurement costs. I estimate a model to analyze the firms' optimal bidding and deployment decisions under cost uncertainty. Using the auction and post-award deployment data, I recover the cost distribution of the firms and show how the contract design influences procurement costs and deployment outcomes. The results show that the firms take the option of not deploying under high-probability cost scenarios, which leads to low deployment rates. The counterfactual analysis shows that incentive contracts with optimal selective bid indexing and penalties can significantly improve deployment rates while keeping procurement costs low.
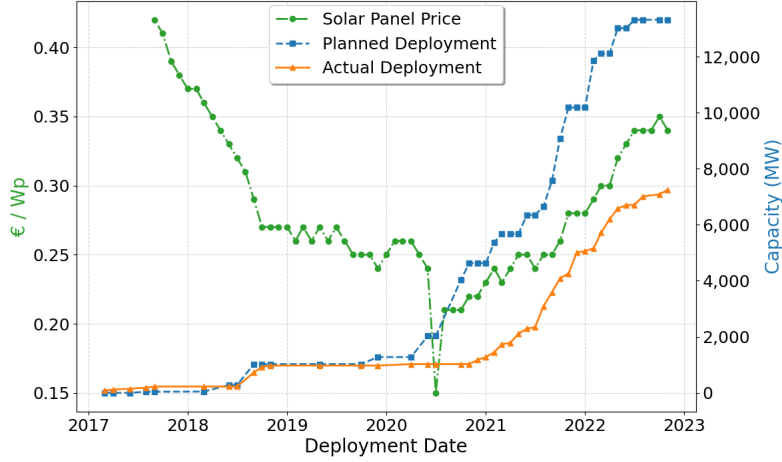
---

1 Introduction

In procurement auctions, contracts set the terms of investment between the governments and firms for the post-auction phase. However, with changes in future conditions, firms may no longer find it optimal to fulfill their investment commitments made at the time of the auction. Failure to define the terms of investments according to future states results in the incompleteness of contracts. Incomplete contracts that do not allow for the revision of the terms of investments based on the future states of the world can lead to under-investment (Hart and Moore (1988), Grossman and Hart (1986)).

In this paper, I discuss how incomplete contracts in renewable energy auctions, which did not include contingencies for future uncertainties, led to the non-deployment of projects. Non-deployment, primarily due to cost uncertainties, poses a significant challenge to achieving the global green energy goals. An annual deployment of 1000 GW of renewable power globally is needed to reach net-zero energy sector emissions by 2050 (IRENA (2023)). I study the case of non-deployment of projects in Indian solar energy procurement auctions. While nearly 22 GW of solar capacity was procured through government-led auctions, only 8 GW had been deployed by 2022. The rising solar panel costs post-2020 resulted in this gap (Figure 1), as firms faced increased costs and delayed or canceled the projects. This highlights the significant challenges in contract enforcement and performance for the green energy transition.

I use a contract design approach with the objective of achieving solar energy goals while minimizing procurement costs under uncertainty. I propose alternative contract designs incorporating two clauses: bid indexing and financial penalties. In bid indexing, firms' final tariffs are adjusted based on the uncertain prices of solar panels, incorporating the risk of price fluctuations and making tariffs contingent on future states of the world. In contrast, penalties are designed to punish firms for non-deployment and make the option of non-deployment costlier for the firms. Using these clauses, I define an incentive contract with three components (McAfee and McMillan (1986), Laffont and Tirole (1987)): first, a fixed component decided during the auctions; second, selective bid indexing, where firms'

final tariffs are adjusted only in cases of cost overruns above a threshold; and third, penalties for non-deployment. I show that this incentive contract enhances cost-effectiveness by encouraging firms to make socially optimal decisions.

Figure 1: Planned vs Actual Capacity Deployment from SECI project status data

In the counterfactual analysis, I compare alternative contract designs by modeling firms' optimal bidding and post-auction deployment decisions. As firms are forward-looking, their optimal bids incorporate expectations of future costs and optimal deployment decisions, including the option to not deploy the projects under high-cost realizations. I then model the dynamic deployment decisions of firms in response to time-varying cost shocks. Using the bid data from auctions and deployment decisions post-award, I recover the firms' cost distribution. I recover this distribution by estimating the primitives of time-invariant private costs, the time-varying solar panel costs, and idiosyncratic cost shocks. These primitives allow me to analyze the effect of contract design on both the bidding and deployment behavior of the firms.

I find that the incentive contract I propose not only performs better than the baseline contract but is more cost-effective than unconditional bid indexing or imposing higher penalties alone, due to having more degrees of freedom in the contract design. The incentive contract achieves a significant 80% increase in deployment with only a 4% increase in tariffs compared to the baseline. This result signifies the role of incentive contracts in achieving

capacity goals while minimizing the increase in tariffs. Unconditional bid indexing results in more than double the 9% increase in tariffs compared to only a 4% increase using the incentive contract to reach the 80% increase in deployment. It is not feasible to increase the deployment by 80% using higher penalties alone. For the same increase of 4% in tariffs, higher penalties lead to only a 40% increase in deployment rates, as compared to almost double the 80% increase in deployment using the incentive contract.

I employ a two-stage model for estimating the primitives. In stage 1, I model optimal bidding to recover bidder types, which are defined by their private costs and capacity. Assuming that all firms share the same expectations regarding solar panel prices and idiosyncratic shocks, any variation in bids is driven by differences in their private costs. Thus, bidder types can be identified through the variation in their bids. These forward-looking firms base their bids on expected profits, taking into account their optimal future deployment decisions.

In stage 2, I use a single-agent dynamic discrete choice model to capture the firm's optimal deployment decisions. The variation in deployment timings helps identify the price coefficient of solar panels and the scale of unobserved idiosyncratic shocks, as these costs influence deployment timing for each bidder type. In each period, firms decide whether to deploy the project or wait until the next period to gain new information about future costs. The firms' decisions to deploy in each period are naturally modeled based on the value derived from deployment and the expected value added from waiting, conditional on not deploying in that period[1]. This means there are states of the world where the firm would have chosen to deploy the project if there were certainty, but due to the uncertainty, they chose to wait[2].

Unlike in a standard first-price auction, in my case, the firms bid below their costs at the

---

[1]This is defined as the quasi-option value, as introduced by Arrow and Fisher (1974), due to the irreversible investments and the net benefit from deployment being dependent on the expected benefits from waiting. This effect is similar to risk aversion, as there is a reduction in the net benefits from deployment due to the benefits of waiting. Even under risk neutrality, the firms behave similarly to risk-averse entities because the benefits of waiting reduce the net benefits of deployment.

[2]This can be interpreted as, if they are uncertain about the payoff to investment in development, they would err on the side of under-investment, rather than over-investment, since development is irreversible (Arrow and Fisher (1974)).

time of auction. This markdown reflects their expectations of decreasing solar panel prices and the option to deploy only in favorable future scenarios. As a result, these markdowns capture firms' expectations of future costs and the option value of deployment. The mean cost at the time of auctions fell from 2.75 INR/kWh in 2017 to 2.59 INR/kWh in 2019 but then rose to 2.69 INR/kWh in 2021. These fluctuations affected bidding strategies, with more aggressive markdowns observed in 2017 and 2021 due to expectations of lower future panel prices. These markdowns often result in firms planning not to deploy under likely cost realizations, which contributes to lower deployment rates. For instance, I find that 80% of projects would be deployed when costs fall below 2.50 INR/kWh, despite only 40% of cost realizations being below that threshold.

I further perform comparative statics to assess how alternative contract designs influence deployment rates and procurement costs. The results indicate that indexing bids to solar panel prices improves deployment rates, especially under conditions of high cost uncertainty, as it reduces firms' risk exposure. However, this approach comes with a trade-off, leading to a significant increase in procurement costs, as firms incorporate future price fluctuations into their bids. On the other hand, contracts that emphasize penalties for non-deployment tend to keep procurement costs relatively lower, as firms are incentivized to follow through on their commitments. However, these contracts are somewhat less effective at driving higher deployment rates, particularly in cases of significant price volatility. Whereas, incentive contracts, where the bids are indexed only in the case of cost overruns, strike a balance by maintaining relatively high deployment rates while keeping procurement costs lower, as firms are encouraged to deploy only when it is socially optimal to do so. Overall, these findings highlight the importance of tailoring contract designs to the level of uncertainty in the procurement setting, balancing procurement costs with the goal of maximizing deployment.

The first contribution of this paper is to the empirical literature on the design of incomplete contracts. My paper is closely related to Herrnstadt et al. (2024), which focuses on the effect of primary deadlines and moral hazard on the surplus of the procurement entity. However, instead of focusing on the moral hazard problem, I primarily focus on the contract

design in the presence of uncertainty and incentivizing the optimal waiting of the firms. It adds to the empirical literature on contract design and the effects of contract design on post-auction actions of the bidders (see Bhattacharya et al. (2022), Lewis and Bajari (2011), DeMarzo et al. (2005)). It also contributes to the empirical application of theoretical literature on the mechanism design approach for optimal incomplete contracts (Hart and Moore (1988), Battigalli and Maggi (2002), Tirole (1999)) and optimal contracts in asymmetric and incomplete information (Laffont and Tirole (1986), Laffont and Tirole (1987), McAfee and McMillan (1986)).

The second contribution of this paper addresses the hold-up problem in the green energy transition caused by incomplete contracts. The hold-up problem arises due to parties hesitating to commit to relationship-specific investments when contracts do not incorporate future contingencies and fail to incentivize optimal relationship-specific investments. Designing contracts to incentivize the parties to honor their investment commitments is a crucial aspect of contract enforcement, especially in developing countries. Contract enforcement remains important in India for the pro-competitive markets in power production (Ryan (2020)). Also, the counterparty risks due to non-compliance of power buyers to honor the contracts create hold-up risks for the green energy transition in India (Ryan (2021)). For the goods where relationship-specific investments are important, countries with good contract enforcement achieve specialization as compared to the other countries (Nunn (2007)). The investments in power generation are very relationship-specific and rely more upon the longer commitment at the contract execution stage than on repeated bargaining (Joskow (1987)). In the cases where parties must make investments based on future states of the world, in general, the first best is not possible (Hart and Moore (1988)). In general, it is too costly or infeasible to define all the contingencies and investments mapped to these contingencies resulting in incomplete contracts. The incomplete contracts give firms an option to renege, delay, and cancel the investments when a third party (courts) cannot verify the details from the contracts. The incomplete contracts might result in inefficiency and under-investment (Klein et al. (1978)). The incompleteness in contracts can show in two forms: discretion,

where the parties don't contract the contingencies with precision, and rigidity, where the contingencies are not contracted sufficiently. Whether to have more contingent clauses or more rigid clauses depends on the level of uncertainty (Battigalli and Maggi (2002)).

The third is a methodological contribution to assess the performance of green energy projects under cost uncertainty using a dynamic discrete choice model. To the extent of my knowledge, this is the first paper that analyzes the performance of renewable energy projects procured through the auctions, where the post-award dynamic decision-making of the firms is involved. This methodology is inspired by the dynamic drilling decisions in the oil drilling literature (Bhattacharya et al. (2022),Herrnstadt et al. (2024) and Kong et al. (2022)). In this stage, firms decide when and whether to deploy the projects within the stipulated time.

The rest of the paper is structured as follows. Section 2 discusses the institutional context of the Indian renewable energy auctions. Section 3 details the data used in the analysis. In Section 4, the model is presented, followed by the solution approach. Section 5 focuses on the identification and estimation of the primitives of the model. Section 6 presents the results, including an analysis of bidder types, uncertainty in costs, and the option of deployment. Section 7 discusses the counterfactual contract design for capacity targets, including incentive contracts with penalties and a baseline analysis for these contracts. Section 8 discusses the contract design in a general context, examining alternative contract designs under uncertainty and the quasi-option value of investment. Finally, Section 9 offers the conclusion.

2   Institutional Context

In 2015, India signed the Paris Agreement, a landmark accord that calls on countries to address climate change and limit the rise in global temperatures to below two degrees Celsius. Following this, India submitted its Intended Nationally Determined Contribution (NDC) to the United Nations Framework Convention on Climate Change (UNFCCC), which included the target of 175 GW of renewable energy by 2022 and 40% of electric power installed

capacity from non-fossil fuels by 2030.

In August 2022, India updated its NDC, aiming to achieve about 50 percent of its cumulative electric power installed capacity from non-fossil fuel-based energy resources by 2030. India's goal of 175 gigawatts (GW) of installed renewable energy capacity by 2022 included 100 GW from solar and 60 GW from wind. The updated target aimed to increase the share of non-fossil fuel energy while also reducing emissions intensity per unit of GDP by 33-35 percent compared to 2005 levels.

The clean energy transition in India is being driven by both central and state authorities. The central authorities procure renewable energy primarily through auctions. This paper focuses on the solar energy auctions conducted by the Solar Energy Corporation of India (SECI), a government-owned company responsible for running solar auctions on behalf of the central government to procure power for the states. The following section discusses the details of the auctions conducted by SECI.

2.1 SECI Auctions

The Solar Energy Corporation of India (SECI) is the implementing agency under the Ministry of New and Renewable Energy (MNRE) responsible for inviting bids for the development of solar, wind, and hybrid projects across India, based on standard bidding guidelines issued by the government. SECI acts as an intermediary in the procurement of electricity between project developers and distribution companies (Discoms), entering into Power Purchase Agreements (PPAs) and Power Sale Agreements (PSAs) with them for a period of 25 years. Under this model, SECI provides payment security to developers and assumes responsibility for collecting payments from the Discoms. This payment security mechanism has enhanced the credibility of the agreements, enabling developers to participate confidently in tenders without fearing non-payment for services.

The tariff to be paid to the developer is fixed at a certain rate for the 25-year project
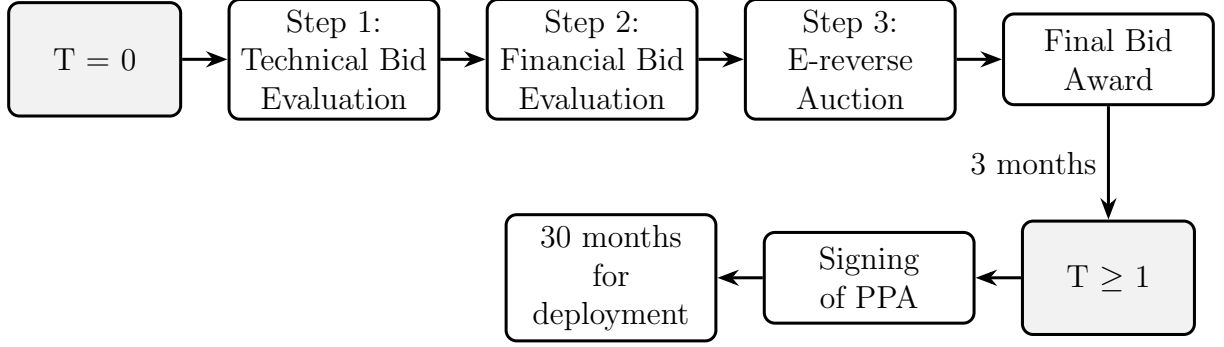
Figure 2: SECI Auction Timeline

period.[3] Solar Power Developers selected through SECI auctions are responsible for setting up Solar PV Projects on a Build, Own, and Operate (BOO) basis in accordance with the provisions of the Request For Proposal (RFP) document and the standard Power Purchase Agreement (PPA).

Figure 2 shows the selection process of the SECI auctions. In step 1, bidders submit their documents to demonstrate that they meet the eligibility criteria outlined in the RFP. In step 2, the bidders are shortlisted based on their bids, as explained in the next paragraph. After this evaluation, shortlisted firms are invited to participate in the e-reverse auction, conducted through an online platform, where the final bid award decision is made.

In step 1, the eligibility of the bids is determined, including ensuring the bid is below the reserve price and meets the technical requirements. In step 2, the financial bid evaluation is a sealed bid round where firms submit a single bid consisting of bid price and capacity. In this step, bidders are shortlisted based on the number of bidders, auctioned capacity, and cumulative bid capacity. The e-reverse auction is a real-time online auction where shortlisted bidders start with the bid price and capacity they bid in the previous step. In this step, bidders compete in an English auction format where they can view the bid prices and capacities of all other bidders, though their identities remain confidential. The minimum permissible decrement in the bid price is 0.01 INR per kWh, and bidders are only permitted

---

[3]Initially, developers were provided with a Viability Gap Fund (VGF) based on their bids, with an upper limit for VGF set as a percentage of the project cost. However, this was discontinued after the initial auctions.

to keep their bid price the same or decrease. Upon completion of this process, bidders are ranked in ascending order based on the tariffs discovered during the auction. Those with the lowest tariffs are declared winners, provided that the cumulative capacity does not exceed the auctioned volume.

After the final award decision, winning bidders are issued a Letter of Award (LoA). The selected bidders are then required to sign the Power Purchase Agreement (PPA) within 3 months of the issuance of the LoA. Before signing the PPA, bidders must submit a bank guarantee, which will be forfeited if the projects are not deployed on time or are canceled. I will refer to this as the penalty for non-deployment in this paper. From the time of signing the PPA, firms have 30 months to deploy the projects as per the PPA.

3   Data

The primary source of data for this paper is the publicly available data on SECI's website. I use the auction data of 33 solar auctions conducted by the central government agency SECI from the year 2015-2021 to procure 21 GW of solar energy capacity. I have the bids of all 196 projects (winners and non-winners) for both the rounds of the auctions, financial bid opening, and e-reverse auctions. The bid data contains the bidder identity, tariff (INR/kWh), and capacity(kW) bid/won by the bidders. Mean bids over the period of 2017-2021 have decreased from 2.66 INR/kWh to 2.45 INR/kWh and the standard deviation of bids has decreased over time.

For the post-auction progress of the awarded projects, I use SECI deployment status data on the capacity deployed across time at the monthly level as of November 2022. This data contains the Power Purchase Agreement (PPA) Date, deployment date, and location of the projects. Deployment timings and Expected vs Actual capacity deployed can be seen in Figure 1. This graph also shows the evolution of the solar panel price index over time taken from monthly wholesale prices for crystalline solar panels by Solarserver in cooperation with pvXchange.

Table 1: Summary Statistics for Solar Auctions by Year

		2017	2018	2019	2020	2021
Auctions	Count	5	4	7	2	3
Allotted Capacity (MW)	Sum	2320	4100	6436	3200	3585
Bidders per Auction	Mean	10.40	8.25	4.29	8.50	10.50
	SD	4.83	2.50	1.50	0.71	4.95
	IQR	6.00	2.25	2.00	0.50	3.50
Tariff (INR/kWh)	Mean	2.66	2.62	2.58	2.46	2.45
	SD	0.37	0.13	0.08	0.09	0.21
	IQR	0.50	0.20	0.09	0.14	0.41
Capacity per Bidder (MW)	Mean	210	322	279	405	406
	SD	142	293	250	253	328
	IQR	200	37	190	200	325
Alloted Capacity per Bidder (MW)	Mean	45	120	214	188	110
	SD	102	183	213	179	178
	IQR	12	250	260	300	250

Note: The table summarizes statistics for solar auctions from 2017 to 2021. Auctions from 2015 to 2016 are omitted here as they had the Viable Gap Funding (VGF) scheme and hence, tariffs per unit output are calculated by getting the discounted value of VGF per unit output.

4 Model

I closely follow the two-stage model of Bhattacharya et al. (2022), where bidding and deployment decisions are made under uncertainty. In the first stage, before the auction, firms draw a private cost type, based on which they decide whether to enter the auction process and what to bid. The second stage is the deployment stage, where, if they win, they have $\bar{T}$ months to commission the project, after which the PPA for non-deployed capacity is terminated.

Let $\mathbb{N}$ be the set of all potential bidders in the market. Before each auction, all firms $i \in \mathbb{N}$ draw a type $(c_{i0}, q_i) \sim \mathcal{F}$, where c_{i0} is the private cost signal, and q_i is the capacity they can deploy. The capacity factor is assumed to be constant across projects and auctions for the

period considered in the paper.[4] For simplicity, in the rest of the paper, q_i will be adjusted for the effective output from the project (i.e., the capacity factor times the capacity). The types are assumed to be private information, independently and identically distributed.

In round 1, bidder i submits a single bid consisting of the bid price b_i^1 (INR/kWh) and capacity q_i (kWh). I assume that each firm bids the maximum capacity. Next, shortlisted bidders enter round 2, a real-time online auction where the bidders open with their bids from round 1 and can either keep their bid prices the same or decrease them. Bidders can observe the bids of all competitors (with identities masked) and their winning capacity at the current bid price. Bidder i's final bid is denoted by (b_i, q_i), and the final award decision by (b_i, q_i^e), where e stands for the e-reverse auction. The auctioned volume is known to the firms before bidding.

Suppose the government seeks to procure quantity Q in the auction. The capacity awarded to bidder i, q_i^e, is given by:

$$
q_i^e = \begin{cases} 0 & \text{if } Q - \sum_{j \neq i} q_j \mathbb{I}[b_i \geq b_j] \leq 0, \\ Q - \sum_{j \neq i} q_j \mathbb{I}[b_i \geq b_j] & \text{if } 0 < Q - \sum_{j \neq i} q_j \mathbb{I}[b_i \geq b_j] \leq q_i, \\ q_i & \text{if } q_i < Q - \sum_{j \neq i} q_j \mathbb{I}[b_i \geq b_j]. \end{cases} \tag{1}
$$

After the auction, we move on to the second stage, the deployment stage. For the decision of when or whether to deploy, time is discrete and denoted by $t \in \{0, ..., \bar{T}\}$, where $\bar{T}$ is 24 months.[5] The contract is set at $t = 0$, and starting at $t = 1$, the firm can decide whether to deploy the project. In each time period t, the firm decides whether to build the project ($d_t = 1$) or not ($d_t = 0$). Firms have $\bar{T}$ periods to deploy the projects and I assume that the terminal value is the stipulated penalty the firms have to pay for the non-deployment of projects.

---

[4]This assumption is based on two observations: first, almost 80% of the projects are planned to be deployed in nearby districts of Jodhpur, Jaisalmer, and Bikaner, which have very similar solar irradiation; second, most solar panels in India are imported from China, and I assume that these projects use solar panels of similar efficiency.

[5]Generally, the deadline is 18 months with an allowed extension of 6 months.

The flow payoff of firm i by deploying at time t is given by:

$$\Pi(b_i, q_i^e, c_{i0}, P_t, \nu_{it}) = (b_i - c_{i0} - \beta P_t)q_i^e + \nu_{it}^1 \tag{2}$$

where, for every time t, P_t (INR/kW) is the price index of solar panels, β is the coefficient converting solar panel price for Levelized Cost of Electricity (LCOE) calculation (from per unit capacity cost (INR/kW) to per unit output (INR/kWh)), and ν_t^d is the action-specific idiosyncratic cost shock capturing unexpected transitory drivers of deployment, where the deployment decision $d \in \{0, 1\}$.

4.1 Model Solution

I solve the model by backward induction. I solve the deployment stage to compute the expected valuations of the firms at $t = 0$. Based on these valuations, the firms optimally bid in the auction stage. Details of both stages are discussed below.

4.1.1 Stage 2: Deployment

For each action $d \in \{0, 1\}$, and for all periods $t \geq 1$, an action-specific cost shock ν_t^d affects the firm's per-period payoff. I assume these shocks $\nu_t = \{\nu_t^0, \nu_t^1\}$ are drawn from an independent and identically distributed (i.i.d.) type 1 extreme value distribution with a scale parameter σ. These idiosyncratic cost shocks represent unexpected, transitory factors influencing deployment decisions, such as financing costs and land availability. They also smooth the predicted time path of deployment in the model.

During each period, $1 \leq t < \bar{T}$, the price of solar panels, denoted P_t, and an idiosyncratic cost shock ν_{it} are realized. The firm then decides whether to deploy the project or to wait. If the firm chooses to deploy, its payoff is given by equation 2. If the firm decides to wait, its payoff is $\nu_{it}^0 + \delta \mathbb{E}\left[V^{\tau-1}(b_i, q_i; c_{i0}, P_t)\right]$, where τ represents the remaining number of periods for deployment, and $\mathbb{E}\left[V^{\tau-1}(.)\right]$ is the expected value of waiting, with δ being the discount factor.

To define the maximization problem, I introduce the value function approach. For any period t, when τ periods are remaining, let $V^\tau(b, q; c_0, P_t)$ denotes value function given the optimal deployment decision is made at time t. Then, the value function V^τ is given by,

$$V^\tau(b_i, q_i^e; c_{i0}, P_t) = \max_{d_t}\{d_t((b_i - c_{i0} - \beta P_t)q_i^e + \nu_{it}^1)$$
$$+ (1 - d_t)[\nu_{it}^0 + \delta\mathbb{E}_{\nu,P|P_t}V^{\tau-1}(b_i, q_i^e; c_{i0}, P_{t+1})]\} \tag{3}$$

for all $t \in \{1, 2, ..., \bar{T}\}$ and $V^0(.) = -\text{Penalty}$. The conditional value function for choice d net of ν_{it} and behaving optimally in future:

$$v_d^\tau(b, q; c_0, P_t) = \begin{cases} \delta\mathbb{E}_{P,\nu|P_t}V^{\tau-1}(b, q; c_0, P_{t+1}) & d = 0 \\ bq - c(c_0, P_t)q & d = 1 \end{cases} \tag{4}$$

and, the conditional choice probability of deployment for bidder i is given by $p_1^\tau(b_i, q_i^e; c_{i,0}, P_t|\lambda, \beta)$:

$$p_1^\tau(b, q; c_0, P_t|\lambda, \beta) = \frac{exp(v_1^\tau(b, q; c_0, P_t|\lambda, \beta))}{exp(v_1^\tau(b, q; c_0, P_t|\lambda, \beta)) + exp(v_0^\tau(b, q; c_0, P_t|\lambda, \beta))} \tag{5}$$

The value functions are computed by backward induction (details in Appendix A.2). Then using, eq(5), I write the conditional choice probability of deployment and non-deployment for every period to estimate the primitives (discussed in detail in Section 5). Given the optimal deployment action in stage 2 of the model, firms will form the expected valuation for the auction stage.

4.1.2 Stage 1: Auctions

To solve stage 1, we need to have the expected valuation of the firm i for the bid award (b_i, q_i^e) conditional on the firm's pre-auction signal (c_{i0}), and solar panel price at the time of the auction i.e. $t = 0$ (P_0). The expected value function for bidder i at $t = 0$ is given by,

$$EV(b_i, q_i^e; c_{i0}, P_0) = \mathbb{E}_{\nu,P_1}\left[V^{\bar{T}}(b_i, q_i^e; c_{i0}, P_1)\right] \tag{6}$$

where $V^{\bar{T}}(.)$ represents the value function when $\bar{T}$ periods are remaining for deployment at

the start of the deployment stage.[6]

To derive the equilibrium bidding conditions, I use the monotonicity of bid prices in bidder types in the first round i.e. the financial bid evaluation round. For this, I use Theorem 1 of McAdams (2003),

Theorem 1 *McAdams (2003) Under assumption 3 - 7 , an Isotone Perfect Strategy Equilibrium exists in games of incomplete information.*

I show that under assumption 1, my setup satisfies the assumptions 3 - 7 of Theorem 1 in McAdams (2003) for the existence of isotone equilibrium. The proof and discussion on the uniqueness of equilibrium in the context of my setting are discussed more in detail in Appendix A.3.

Assumption 1 $EV(.)$ *as defined in eq(6) satisfies non-decreasing differences in (b_i, t_i) and is supermdoular in b_i, where $t_i = (c_{i0}, q_i)$ is the bidder type.*

Using Theorem 1, for the equilibrium bidding in the first round of auction ensures that only the highest types reach the second round, which enables me to use order statistics to write down the likelihood of the observed bids using the optimal bidding conditions.

Further, to derive the equilibrium bidding condition for the second round i.e. the e-reverse auction, I make the following assumption:

Assumption 2 *Auction's procuring procedure for the second round follows Milgrom and Weber (1982) clock model of an English auction.*

Following Donald and Paarsch (1996) and assuming the clock model of Milgrom and Weber (1982), equilibrium bidding states bidders do not exit the auction till their expected valuations have reached zero and exit when the bids decrease such that expected valuations are below zero. Hence, the following are the equilibrium bidding conditions,

---

[6]Generally there is a three-month gap between the auction and deployment stage. Hence, P_0 is the solar panel price at the start of the auction stage ($t = 0$) and P_1 is the solar panel price at the start of the deployment stage ($t = 1$)

$$EV(b_{nw}^*, q_{nw}^e; c_{nw,0}, P_0) = 0 \tag{7}$$

$$EV(b_w^*, q_w^e; c_{w,0}, P_0) = b_m^* \tag{8}$$

where, $nw \in \mathcal{N}^{nw}$, $w \in \mathcal{N}^w$, and $m \in \mathcal{N}^m$. Here, $\mathcal{N}^{nw}$, $\mathcal{N}^w$, and $\mathcal{N}^m$ are the sets of non-winning, winning, and marginal bidders respectively.

Following Milgrom and Weber (1982) as the equilibrium bidding strategies at English and Vickrey auctions are given by eq(7)-(8), deriving the likelihood function for estimation is straightforward (discussed in detail in 5).

Given, that we now know how to write down the likelihood function of the observed bids and deployment decisions, I will discuss the identification strategy and estimation of the primitives of the model.

5 Estimation

In this section, I will describe the identification strategy and estimation of the two-stage model. This will be followed up with the parametric assumptions to estimate the model's primitives. The identification and estimation are divided into three parts: first, estimating the bidder types from the first stage of the model; second, identifying the coefficient of solar panel prices and idiosyncratic shocks from the second stage; and third, separately estimating the stochastic price process of solar panel prices.

The parameters of interest are given by $\Lambda, \Gamma, \Upsilon$, where Λ are the parameters of the distribution of bidder types $((c_0, q))$, Γ are the parameters of price coefficient of the solar panel (β) and scale of idiosyncratic shocks (σ), and Υ the parameters of the stochastic price process. In the following sections, I will discuss how the likelihood functions are set for the above three parts to estimate the parameters of the model and the identification strategy.

5.0.1 Likelihood of Bids

I will define the likelihood function for the observed bids using the bids from the second round and the order of bids from the first round. For the second round, an ordered sample of p bids has $n - p$ non-participants and p participants:

$$B_{(1:n)} \leq B_{(2:n)} \leq \cdots \leq B_{(p:n)}$$

with the k winners and let $B_{min} \sim \mathcal{G}$, where $EV(B_{min}, q, c_0, P) = 0$ and B_{min} is the break-even bid. Under the assumption of $EV(\cdot)$ satisfying non-decreasing differences in (b_i, t_i), where $t_i = (c_{i0}, q_i)$ is the bidder type, the bidder with the lower break-even bid is of the higher type (details in the Appendix A.3).

Hence, to calculate the likelihood of the observed bids, we need the winners' cumulative density functions and order statistics. Correspondingly, we need the probability density functions and order statistics for the participating non-winning bidders.

For the winners, we need the cumulative density of the order statistic, and the winners are ordered based on their bids in the first round, following Theorem 1. The Cumulative Density Function (CDF) of the (k)th is given by:

$$G_{(k,n)}(b|\Lambda, \Gamma) = \sum_{j=k}^{N} \binom{N}{j} G(b|\Lambda, \Gamma)^j (1 - G(b|\Lambda, \Gamma))^{N-j}$$

For the non-winners, we need the probability density of the order statistic, and the bidders are ordered based on their bids in the second round. The Probability Density Function (PDF) of the (k)th order statistic is:

$$g_{(k,n)}(b|\Lambda, \Gamma) = n \binom{N-1}{k-1} G(b|\Lambda, \Gamma)^{k-1} (1 - G(b|\Lambda, \Gamma))^{(n-1)-(k-1)} g(b|\Lambda, \Gamma)$$

To calculate the distribution for all bidders, I will use simulated maximum likelihood as we cannot point-identify the private cost signals of the winners using the equilibrium

conditions for optimal bidding. I can still calculate the maximum private cost signal for each winner given their bids; hence, I will integrate over the range of possible cost signals. The joint distribution of the bids for auction a is given by:

$$LL_b^a = \int^{c_{w0,max}} \left(\sum_{i=1}^{k} \ln(g_{(i,n)}(.)) \right) f(cw0|\Lambda) dc_{w0} + \sum_{i=k+1}^{p} \ln(g_{(i,n)}(.)) \tag{9}$$

where $c_{w0} = \{c_{10}, c_{20}, \ldots, c_{k0}\}$ and maximum signals for winners is given by $c_{w0,max} = \{c_{10,max}, c_{20,max}, \ldots, c_{k0,max}\}$.

The identification of the parameters of the distribution of bidder types relies on the variation across bids, which is primarily due to the variation in the private costs drawn by the bidders, given that in a particular auction, all bidders observe the same price of solar panels.

Given that in the second round, the bid function for the non-winners is effectively an identity function as shown in eq(7), the assumption of bidder types distribution $\mathcal{F}$ is effectively an assumption on the distribution of bids. If given the distribution of $\mathcal{F}$, we can write the distribution of the observed bids and identification of parameters is assured by the assumption of $\mathcal{F}$ (Donald and Paarsch (1996)).

5.1 Likelihood of Deployment

Given the value function approach, we can calculate the conditional choice probability for every time period for the single-agent dynamic discrete choice problem. For period t, when τ periods are remaining, the conditional choice probability of deployment for bidder i is given by $p_1^\tau(b_i, q_i^e; c_{i,0}, P_t|\Lambda, \Gamma)$ (details in the appendix **??**).

$$p_1^\tau(b, q; c_0, P_t|\Lambda, \Gamma) = \frac{1}{1 + \exp[v_0^\tau(b, q; c_0, P_t|\Lambda, \Gamma) - v_1^\tau(b, q; c_0, P_t|\Lambda, \Gamma)]} \tag{10}$$

For auction a, the log-likelihood equation for all winners $i \in \mathcal{N}_w^a$ is:

$$\sum_{i=1}^{N_w^a} \left[\sum_{\tau=\tau_i^e+1}^{\bar{T}} (\ln(p_0^\tau(b_i, q_i; c_{i0}, P_{\bar{T}-\tau+1i}|\Lambda, \Gamma))) + \ln(p_1^\tau(b_i, q_i; c_{i0}, P_{\bar{T}-\tau+1i}|\Lambda, \Gamma)) \right] \qquad (11)$$

where τ_i^e are the time periods left when the project gets deployed and equal to 0 when it never gets deployed.

As we can only observe the upper bound of the signal for the winning bidders, using SMLE, the log-likelihood is given by:

$$LL_d^a = \sum_{i=1}^{N_w^a} \left[\int^{c_{i0,max}} \sum_{\tau=\tau_i^e+1}^{\bar{T}} \left((1 - d_i^\tau) \ln(p_0^\tau(b_i, q_i; c_{i0}, P_{\bar{T}-\tau+1i}|\Lambda, \Gamma)) \right. \right.$$

$$(12)$$

$$\left. \left. + d_i^\tau \ln(p_1^\tau(b_i, q_i; c_{i0}, P_{\bar{T}-\tau+1i}|\Lambda, \Gamma)) \right) f(c_{i0}|\Lambda) dc_{i0} \right]$$

where $c_{i0,max}$ is the upper bound of the cost signal.

The identification strategy for this likelihood function leverages that private cost signals for every winning bidder would remain constant in the deployment, and the only variables realized in each period would be the solar panel prices and the idiosyncratic shocks. Solar panel prices and idiosyncratic shocks play a significant role in determining the net value of deployment. The model assumes that the decision to deploy is based on the net benefit compared to waiting. The assumption that private cost signals remain constant during the deployment period allows us to isolate the effect of solar panel prices and idiosyncratic shocks on deployment decisions, given the cost signals.

The identification strategy employs Conditional Choice Probabilities (CCPs), denoted as $p_1^\tau(b_i, q_i; c_{i0}, P_t|\Lambda, \Gamma)$. CCPs reflect the probability of deployment given the state and model parameters. By linking observed choices to these CCPs, we can estimate the structural parameters Λ and Γ (Hotz and Miller (1993)).

The likelihood function is constructed from observed choices and CCPs. The integral

over the upper bound of the cost signal accounts for the unobservable nature of the true cost. Using SMLE, the likelihood function captures the distribution of cost signals and their impact on the firms' deployment decision (Arcidiacono and Miller (2011)).

5.2   Estimation Algorithm

The algorithm I have proposed for estimating the parameters Γ and Λ is fundamentally inspired by the Expectation-Maximization (EM) algorithm, as introduced by Dempster et al. (1977). The EM algorithm uses the iterative method designed to leverage the variation in data by iteratively maximizing the likelihood function. In their seminal paper, they provided a robust mathematical framework that proves convergence to a local maximum of the likelihood function.

In my estimation algorithm, I utilize the principles of the EM algorithm by alternating between updating Γ and Λ to maximize their respective likelihood functions conditionally. Specifically, the update of Γ given the current estimate of Λ corresponds to the E-step, where the expected log-likelihood involving Γ is maximized. Similarly, the update of Λ given the updated estimate of Γ mirrors the M-step, where the maximization of the expected log-likelihood involving Λ occurs. This iterative process of conditional maximization aligns with the methodology described by Dempster et al. (1977), ensuring that each parameter is optimized given the other, thereby enhancing the overall efficiency and accuracy of the parameter estimates.

The estimation problem involves estimating parameters Γ and Λ using two likelihood functions, LL_d^a and LL_b^a. Here's how the EM algorithm framework applies:

Initialization Start with initial guesses $(\Gamma^{(0)}, \Lambda^{(0)})$.

Step 1 (E-step) Expectation: Compute the expected log-likelihood involving Γ given the current estimate of Λ, $\Lambda^{(m)}$.

This corresponds to the update:

$$\Gamma^{(m+1)} = \operatorname*{argmax}_{\Gamma} \sum_{a=1}^{A} LL_d^a(.|\Lambda, \Gamma^{(m)})$$

Here, I am maximizing the log-likelihood of Γ while keeping Λ fixed.

Step 2 (M-step) Maximization: Given the updated $\Gamma^{(m+1)}$, maximize the expected log-likelihood involving Λ.

This corresponds to the update:

$$\Lambda^{(m+1)} = \operatorname*{argmax}_{\Lambda} \sum_{a=1}^{A} LL_b^a(.|\Gamma^{(m+1)}, \Lambda)$$

Here, I am maximizing the log-likelihood of Λ while keeping Γ fixed.

Iteration Repeat steps 1 and 2 until convergence. This means continuing the alternating maximization until the changes in Γ and Λ between iterations are below a set threshold.

5.3   Stochastic Process of Prices

Following Bhattacharya et al. (2022), I assume that that P_t follows Geometric Brownian Motion (GBM) with parameters $\Upsilon = \{\mu_p, \sigma_p\}$,

$$log(P_{t+\Delta}) - log(P_t) = \left(\mu_p - \frac{\sigma_p^2}{2}\right)\Delta + \sigma_p(\Delta\epsilon_t)^{1/2}$$

where ϵ_t represents the Brownian innovation and thus is distributed standard normal and i.i.d. across time and $\Delta = 1/12$ i.e. 1 month

Using the above equation, we can get:

$$\mathbb{E}log(P_{t+\Delta}) = log(P_t) + \left(\mu_p - \frac{\sigma_p^2}{2}\right)\Delta$$

and then using maximum likelihood, the parameters of the distribution are estimated.

6   Results

This section discusses the structural estimates of the two-stage model and how these estimates affect the firms' bidding and deployment decisions. The analysis is divided into three parts, first discusses the distribution of bidder types and private costs. Second, I present the estimates of solar panel costs and unobserved idiosyncratic costs, which are uncertain and realized in every period of the deployment decision. Third, I introduce the baseline case for counterfactual simulations, which will serve as a reference point for analyzing the alternative contract designs.

By understanding these structural estimates, we can better assess the implications of various contract designs on the procurement process, deployment rates, and overall procurement costs. This sets the stage for the counterfactual analysis, where I will evaluate the trade-offs between increasing deployment and minimizing procurement costs under different contract designs.
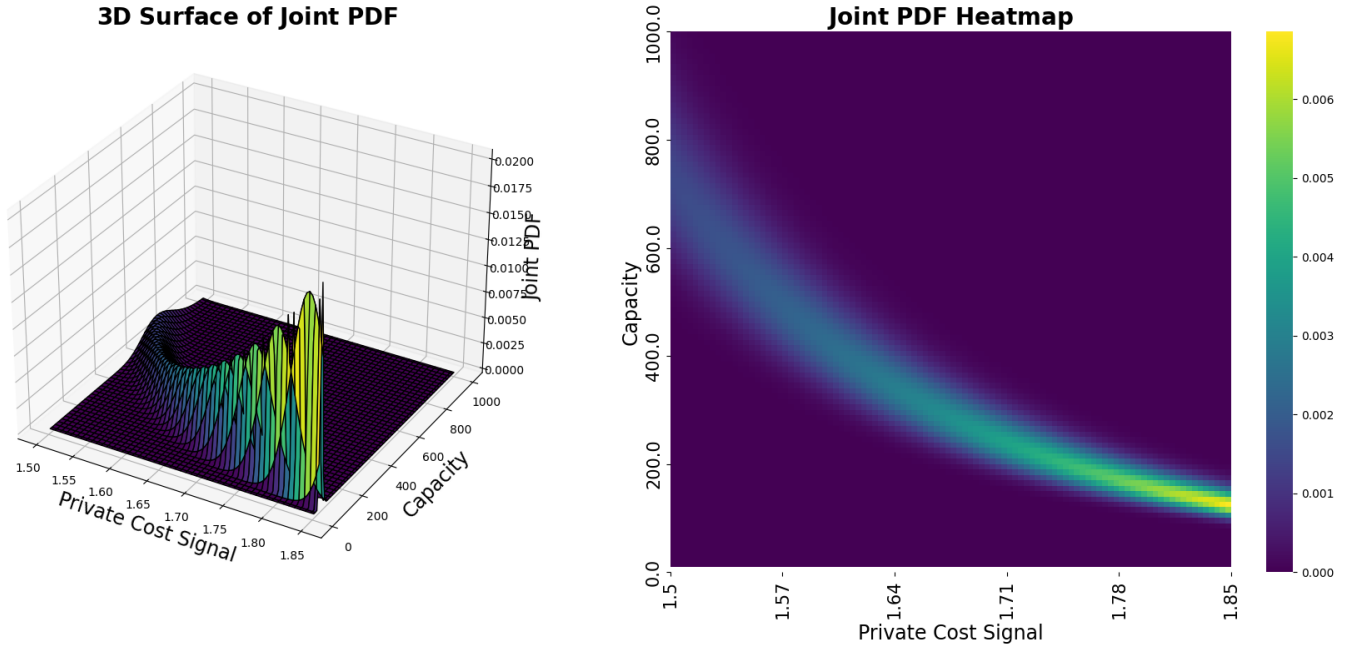
Figure 3: Distribution of bidder types: $(c_0, q) \sim \mathcal{F}$

6.1 Bidder types

The bidder types are defined by the joint distribution of private costs and firm capacity. The bidder type distribution in Figure 3 illustrates a strong negative correlation between the private costs and firm capacity: firms with larger capacities tend to have lower private costs compared to those with smaller capacities (functional assumptions and estimated parameters table in Appendix A.4). Additionally, the figure shows a high density of small and mid-capacity firms in the auctions and a relatively lower density of high-capacity firms.

Estimating the bidder-type distribution allows me to recover the expected costs of the firms that won the bids. Given the auction format and subsequent equilibrium conditions, we can only recover the maximum private cost signal for the winning firms using the estimated parameters. Knowing the distribution of bidder types, we can use the maximum private cost signal to calculate the mean cost and confidence bands for the winning firms at solar panel prices prevailing at the time of the auctions, as shown in Figure 4. I observe that the tariffs are below the costs when calculated at the solar panel prices at the time of the auctions, indicating that the firms are bidding lower than their costs at the time of the auctions. In the next section, I will discuss these 'markdowns' due to the uncertainty in solar panel prices and firms having the option value of deployment.

6.2 Uncertainty in Costs and Option of Deployment

In this section, first I discuss the markdowns at the time of the auctions due to the uncertainty in costs and the option of deployment. Second, to show the reason behind the low deployment rates, I use the estimated parameters of the model to simulate the expected costs of the winning firms for the second stage and analyze deployment decisions under these costs.

To illustrate the effect of cost uncertainty and decompose the effect of the uncertain solar panel prices and option value of deployment, I simulate bids and the corresponding expected costs at the time of the auction for a single firm to see the markdowns at the break-even bids.

Figure 5 depicts the expected costs (a) if it did not change from $T = 0$ (green), (b) if solar panel prices were constant, uncertainty was only due to idiosyncratic shocks and firms have the option whether to deploy or not and (c) uncertainty due to idiosyncratic shocks and solar panel prices and firms have the option whether to deploy or not (purple). If there was no uncertainty and the firms did not have the option of deployment, the expected costs would just be constant (green curve). Whereas if the firms can wait to see the idiosyncratic shocks and then choose whether or not to deploy, the expected costs (red curve) and the break-even bids decrease as firms choose only to deploy in favorable states of the world. Similarly, with the expectations of a decrease in solar panel prices, the expected costs (purple curve) and break-even bids decrease even further.
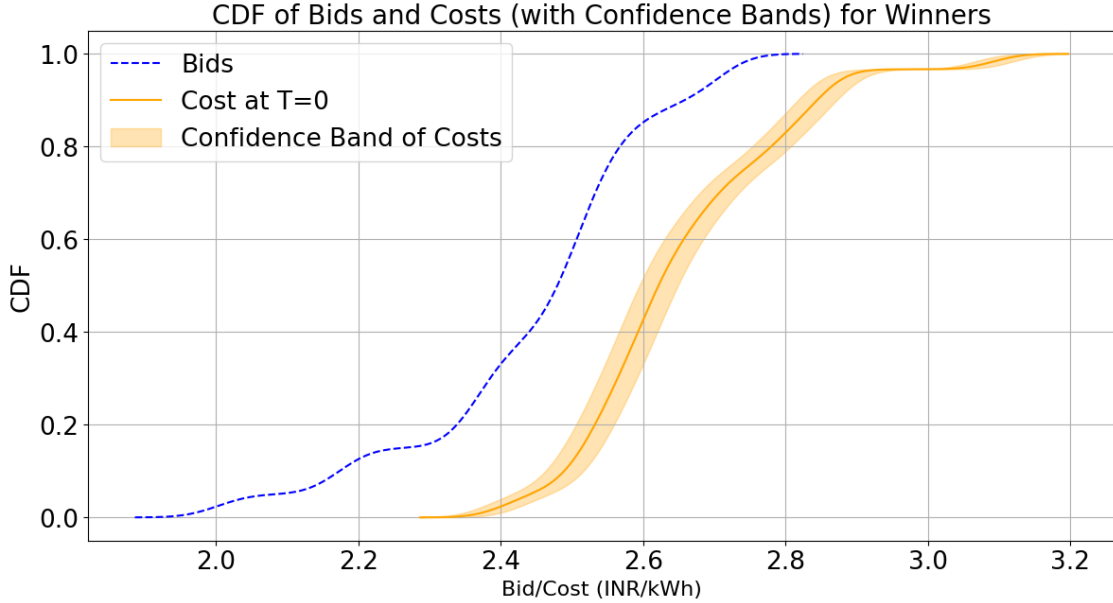

Figure 4: CDF of tariffs and expected costs for the winning firms. **(i)** The Blue line shows the tariffs of the projects by the winning firms **(ii)** As for the winners, we can only back out the maximum value of c_0, the orange line shows the expected value of costs calculated at solar panel prices at $T = 0$ and the shaded area shows 95% confidence bands, given distribution of c_0 conditional on capacity, maximum value of c_0. The curves were smoothed using kernel density estimation.

These markdowns illustrate that the firms bidding close to their break-even bids only take the option to deploy when they see the favorable states of the world and actual profits are positive. In high-cost realizations, firms have negative profits and would take the option

to not deploy and pay the penalties.

Next, I simulate the costs for the winning firms to analyze the deployment decisions of the firms. In Figure 6, the expected costs of the firms over periods up to the deadline are shown, with the red curves indicating the costs at which the projects were deployed in the simulations. These simulations reveal that in some of the lower-density parts of the expected cost curves, there is a higher density of project deployments. Conversely, as we move towards the higher-cost areas on the right, the probability of deployment decreases. Hence, firms plan to deploy their projects with a high probability when future cost realizations are low and with a low probability when cost realizations are high. However, there is heterogeneity in firms' deployment decisions due to the presence of private costs. This heterogeneity explains why in some cases the deployment occurs even in some high-cost realizations.
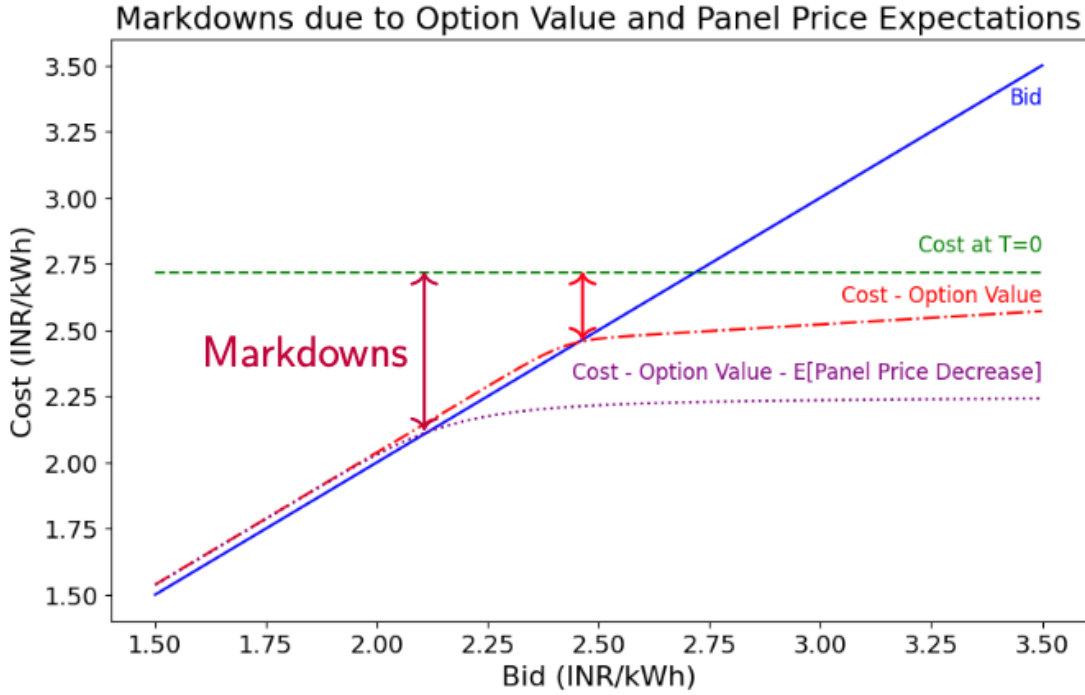
Figure 5: Expected Costs under uncertainty and option of deployment. The expected cost per unit is calculated by subtracting the expected profit per unit output from the bid. This figure illustrates how the cost curves shift due to these factors for the where capacity is 150 MW and c_0 is 1.6 INR/kWh

The simulations show significant differences in cost components between projects that were deployed and those that were not. For deployed projects, the average share of com-

mon costs is notably lower at approximately 25.65%, compared to 38.28% for non-deployed projects. As perceived deployed projects tend to have a smaller proportion of common costs relative to the total cost. Conversely, the share of idiosyncratic shocks is higher in deployed projects, averaging 5.25%, compared to 1.23% for non-deployed projects. These findings show the distribution of average cost components on project deployment, with deployed projects showing a higher relative contribution from idiosyncratic shocks and a lower proportion of common costs.
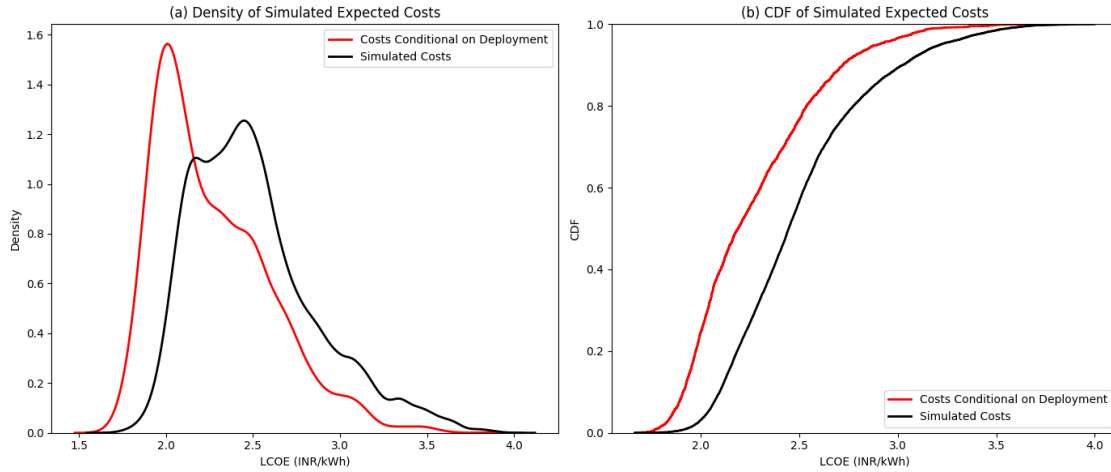
Figure 6: The black curves represent the simulated expected costs for the winning firms, while the red curves indicate the expected costs conditional on the actual deployment times of the projects in the simulations.

The above results show that under cost uncertainty and low penalties, firms decide not to deploy projects when favorable conditions are not realized. This led to delays and cancellations of projects and firms not honoring their investment commitments. Therefore, contract design must address these issues for India to achieve its capacity goals.
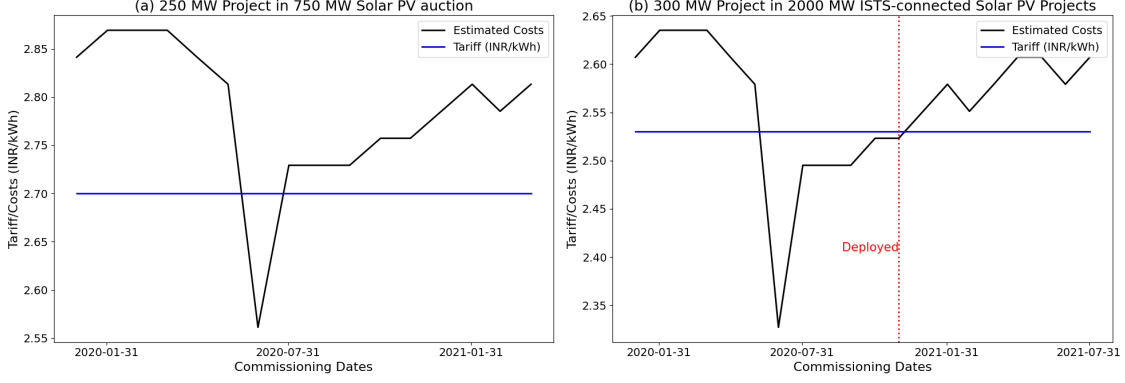
Figure 7: The estimated costs of two projects for example. (a) 250 MW project which was not deployed after the cost shock. (b) 300 MW project that was deployed after the cost shock. The costs are estimated using the estimated parameters and simulation of idiosyncratic shocks with actual solar panel price realizations

6.3 Baseline Analysis

For the counterfactual analysis of tariffs, we need to establish baseline tariff rates that vary over time, reflecting changes in the expected costs based on the then-current prices of solar panels. Therefore, the baseline tariffs and costs used for the counterfactual simulations are shown in Figure 8. The closeness of tariffs to costs at the time of the auction indicates the extent to which firms are marking down their bids to account for expected future cost decreases and the option of deployment.

Estimates indicate that the mean cost at the time of auctions decreased from 2.75 INR/kWh in 2017 to 2.59 INR/kWh in 2019, but then rose to 2.69 INR/kWh in 2021. The average percentage markdown was most pronounced in 2017 at -18.40%, driven by expectations of lower panel prices and aggressive bidding. This markdown decreased to -0.23% in 2019 due to a lower baseline for panel prices and less aggressive bidding. In 2021, the markdown increased again to -15.83%, as firms anticipated higher prices due to an elevated baseline. These trends reflect the firms' evolving bidding strategies in response to panel prices and competitive dynamics.
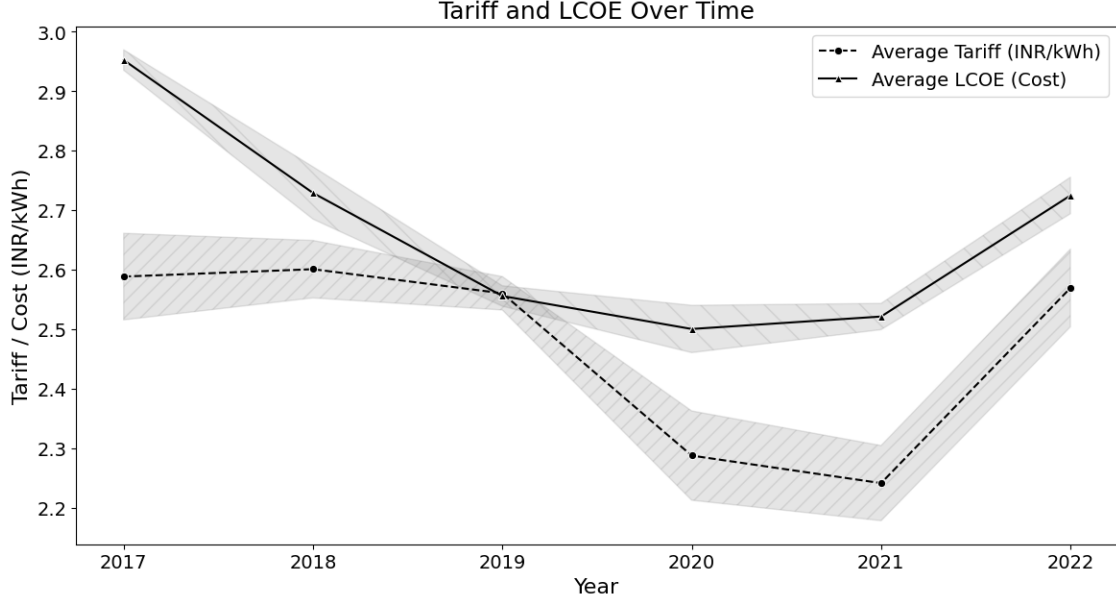
Figure 8: Tariffs and Estimated costs of the participant firms over time. (a) The blue line shows the actual average tariffs. The red line shows the average costs of all firms participating in the auctions.

To evaluate the trade-off between increasing deployment and lowering tariffs, and to assess the cost to the government for boosting deployment rates from the current level, I will compare the tariffs in counterfactual scenarios to the baseline tariff rates.

7 Counterfactuals

This section explains how I determine the optimal parameters for the incentive contract with selective bid indexing and penalties, based on the set of estimated primitives. The analysis is divided into three parts. First, I define the government's optimization problem. Second, I describe the alternative contracts used in the analysis. Third, I identify the optimal parameters for the incentive contract.

7.1 Contract Design for Capacity Targets

The central government of India introduced these auctions to meet its green energy goals. It has also set renewable energy targets for the state governments, which are the majority of

the electricity buyers. The state distribution companies have Renewable Purchase Obligations (RPOs) which have to procure a certain proportion of the total energy from renewable energy sources. Therefore, in this paper, I will assume that the central government has a fixed target for every and is procuring green energy accordingly. Hence, I will compare the contract designs by evaluating procurement costs to ensure they achieve the capacity targets with a high probability.

As discussed in eq **??**, expected value function for bidder i at $t = 0$ is given by,

$$EV(b_i, q_i^e; c_{i0}, P_0) = \mathbb{E}_{\nu, P|P_0} \left[V^{\bar{T}}(b_i, q_i^e; c_{i0}, P_1) \right]$$

For every bidder $i \in \mathbb{N}$, given the vector $(b_i, q_i^e; c_{i0}, P_0)$, let the ex-ante probability of deployment of the project be denoted by $Pr(b_i, q_i^e; c_{i0}, P_0)$. Let the total capacity auctioned off be $q = \sum_i q_i$. Then the expected capacity deployed would be $\sum_{i \in \mathbb{N}} q_i Pr(b_i, q_i^e; c_{i0}, P_0)$. The Expected procurement cost in terms of tariff (INR per kWh) per unit capacity (kW) deployed would be,

$$EPC = \frac{\sum_{i \in \mathbb{N}} b_i q_i^e Pr(b_i, q_i^e; c_{i0}, P_0)}{\sum_{i \in \mathbb{N}} q_i Pr(b_i, q_i^e; c_{i0}, P_0)} \tag{13}$$

Assuming the first n_e order statistics are the winners of the auction, the auction clearing bid is given by the threshold bid for the $(n_e + 1)$th order statistic. Therefore, the threshold bid for $(n_e + 1)$th order statistic is given by $b_{(n_e+1)}^*$

$$EV(b_{(n_e+1)}^*, q_{(n_e+1)}; c_{0,(n_e+1)}, P_0) = 0$$

In alternate contract designs, to minimize procurement costs while achieving the government's capacity targets, I will determine the optimal parameters for incentive contracts and the optimal penalties based on the model's primitives.

Hence, the optimization problem with capacity target with probability P^{target} :

$$\text{Minimize} \quad EPC$$

$$\text{subject to} \quad \sum_i q_i Pr(b_i, q_i^e; c_{i0}, P_0) \geq P^{target} q \quad \text{and}$$

$$b_i^* = b_{(n_e+1)}^*, \forall i$$

7.2 Alternate contract designs

This section defines three types of alternative contracts aimed at achieving the target capacity: incentive contracts, contracts with unconditional bid indexing, and contracts with penalties. The use of bid indexing and penalties are intended to address markdowns caused by expectations of decreasing solar panel prices and the option value of deployment, respectively (Figure 5). Whereas, incentive contracts, in addition to accounting for these two factors, also incentivize firms to make socially optimal deployment decisions.

7.2.1 Incentive contracts

The incentive contracts bound the benefits of waiting as the government allows the firms to adjust bids for a proportion of cost overruns and cost under-runs. The bid adjustment parameters should be optimally chosen so that firms do not wait too much (lessen the probability of deployment) or wait too little (raise the costs of deployment). To do that, I introduce the adjustment parameters P_u, P_l, κ and define the flow payoff in the incentive contracts as:

$$\Pi(b, q, c_0, P_t, \nu, \kappa, P_l, P_u) = \bigg(\underbrace{\underbrace{b}_{Bid} + \underbrace{\kappa \, \mathbb{I}[P_t < P_l]\beta(P_t - P_l)}_{Under\text{-}runs} + \underbrace{\kappa \, \mathbb{I}[P_t > P_u]\beta(P_t - P_u)}_{Overruns}}_{Final\ Tariff}$$

$$\hspace{5cm} - c_0 - \beta P_t \bigg) q + \nu_t^1 \hspace{2cm} (14)$$

where the incentive contracts have two components: 1) Bid (b): The fixed component of the contract, determined at the first stage, 2) Cost adjustments: under-runs, if the price for solar panels falls below a lower threshold (P_l) the government reduces the tariff by a factor $\kappa\beta(P_t - P_l)$ and overruns, if the price for solar panels exceeds an upper threshold (P_u) the government increases the tariff by a factor $\kappa\beta(P_t - P_u)$. The parameters of the incentive contract can be represented by $\psi^{IC} = \{\kappa, P_l, P_u, -Pen\}$

7.2.2 Contract with unconditional bid indexing

The bid indexing allows firms to index their bids by a factor of *kappa* unconditionally. If we allow firms to index their bids to solar panel prices, we can allow the firms to adjust tariffs to uncertainty. Let κ be the bid index parameter, then the flow payoff of the bidder by deploying at time t is given by:

$$\Pi(b, q, c_0, P_t, \nu, \kappa) = (\underbrace{\underbrace{b}_{\text{Bid}} + \kappa\beta P_t}_{\text{Final Tariff}} - c_0 - \beta P_t)q + \nu_t^1 \tag{15}$$

where the parameter of the unconditional bid indexing contract can be represented by $\psi^{BI} = \{\kappa\}$

7.2.3 Contract with penalties

In this contract, we only impose higher penalties to reach the target capacity. The parameter of the penalties contract can be represented by $\psi^{Pen} = \{-Pen\}$

7.3 Optimal parameters of the alternate contracts

Using the parameters of the alternate contracts, I simulate EPC in equation 13 to find the optimal parameters of a specific contract. If the parameters of a contract are represented by ψ, the optimization problem for this contract design can be written as,

$$\min_{\psi} \quad EPC(\cdot \mid \psi)$$

$$\text{subject to} \quad \sum_i q_i Pr(b_i, q_i^e; c_{i0}, P_0 | \psi) \geq P^{target} q \quad \text{and}$$

$$b_i^* = b_{(n_e+1)}^*(\cdot \mid \psi), \forall i$$

To solve the optimization problem defined for each contract design, I apply a grid search algorithm to find the optimal parameter set ψ for a specified target capacity (P^{target}).

7.4 Alternate contracts vs baseline analysis

I determine the optimal parameters $\psi^{IC}, \psi^{BI}, \psi^{Pen}$ for the three alternative contract designs for each target capacity ($P^{target} = \{50\%, 55\%, ..., 85\%\}$). Using these parameters, we can identify which contract is the least expensive for each target capacity and by how much (Figure 9). My findings show that although bid indexing helps achieve the 80% target, the incentive contract reaches that target with only a 4% increase in tariffs, compared to a 9% increase under bid indexing. Penalties, however, are far less effective in meeting deployment targets, even when increased to eight times their current level. Given the structure of incentive contracts, they can converge to either unconditional bid indexing or penalty-only contracts if those result in the lowest procurement cost. Thus, incentive contracts are more effective in minimizing procurement costs than relying solely on bid indexing or penalties.
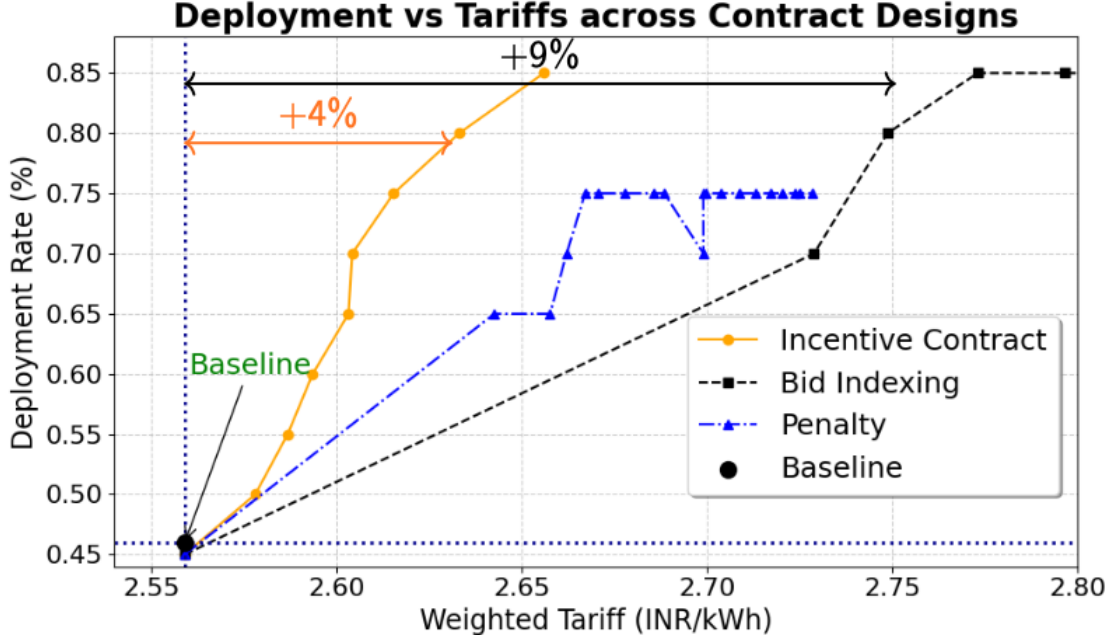
Figure 9: The optimal parameters for the incentive contract were computed for the targets = $\{50\%, 55\%, ..., 85\%\}$. Weighted tariff is the average tariff of projects deployed weighted with the project capacities.

By definition, the incentive contract should be the cheapest of the three, as it would naturally converge to the least expensive option if either bid indexing or penalties were optimal. However, Figure 9 illustrates how much cheaper the incentive contract becomes when we increase capacity targets using optimal selective bid indexing and penalties. Next, I assess the performance of incentive contracts compared to the baseline contract using the actual price path observed in the data.

Similar to Figure 8, I will simulate the baseline analysis according to the current contract design to compare the performance of incentive contracts with the actual contract design. As shown in Figure 10, incentive contract tariffs are initially much higher than costs due to the upper threshold being reached every period because of high solar panel prices, resulting in tariffs being indexed upwards consistently at first. However, as solar panel prices decrease, the tariffs in the incentive contracts also reduce. After 2019, as solar panel prices increase, the tariffs rise again. In contrast, in the baseline analysis, the tariffs remain constant for firms once the auctions conclude. Consequently, deployment rates declined significantly

when there was a positive input cost shock. With incentive contracts, once the shock is realized, firms are allowed to index their bids upwards, leading to increased final tariffs and, subsequently, higher deployment rates.
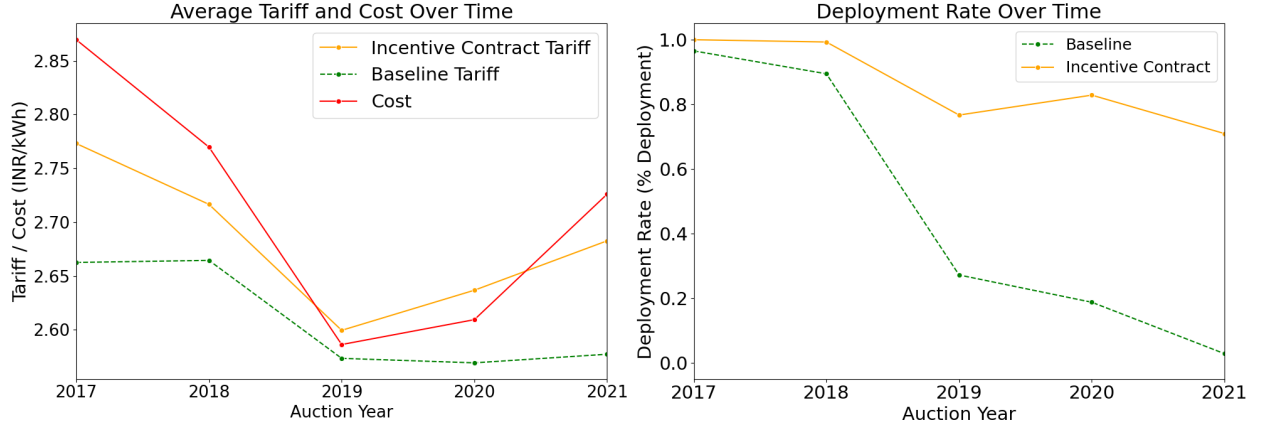
Figure 10: Assuming $\kappa = 57\%$, $P_U = 0.28$, $P_l = 0.1$, $Pen = 10^7$ .The graph compares the tariffs over time in actual contract design (baseline case) vs. incentive contracts. Additionally, the costs over time are also plotted to compare the markdowns across both contract designs.

The deployment under incentive contracts is 83%, compared to 47% in the baseline case. This 56% increase in deployment results in higher tariffs for the incentive contracts. The weighted average tariff for deployed projects under incentive contracts is 2.73 INR/kWh, compared to 2.55 INR/kWh in the baseline case. This 7% increase in tariffs is primarily driven by higher solar panel prices and increases in tariffs of 9% and 13% for incentive contracts in 2020 and 2021, respectively, compared to the baseline.

8 Comparative Statics and Discussion

This section discusses how the contracts can be designed to increase the deployment and achieve capacity targets while minimizing procurement costs in a more general way. The last section primarily focused on the optimal contract parameters given the estimated primitives for the case of India. However, in this section, I will discuss how different contract parameters affect the deployment rates and procurement costs.

By analyzing the firms' optimal bidding and deployment decisions, we can observe the

effect of various contract features on deployment rates and procurement costs. I will consider two sets of analyses to assess their effects. First, I will focus on the impact of contract clauses under different levels of uncertainty in solar panel prices. Second, I will examine how the contract clauses influence the deployment timing of firms, and consequently, the deployment rates and bid prices.

## 8.1 Contract design under uncertainty

I find that as uncertainty increases, incorporating more contingent clauses is more beneficial than relying on the rigid clauses [7]. Specifically, indexing the bids proves to be more effective than imposing higher penalties for increasing the deployment. Conversely, when uncertainty is reduced, higher penalties become more effective in keeping the prices down than bid indexing. I introduce uncertainty in terms of price volatility in solar panel prices. Subsequently, I analyze the impact of these contract clauses on the bid prices and deployment. The bids will be indexed to the solar panel prices to observe the effects of contingent clauses. For rigid clauses, the penalties will be imposed for non-deployment.

First, I will consider the effects of price volatility on solar panels. As the volatility increases, I find that the penalties are less effective in increasing the deployment. To illustrate this, I show two cases of penalties; one where the penalties are low (half of the current penalty) and the other where they are very high (eight times). As shown in Figure 11, higher penalties are relatively less effective in increasing the deployment as compared to lower penalties when the volatility increases. At higher levels of volatility, firms' markdowns are more influenced by the expectation of lower future solar panel prices than by the impact of higher penalties, making penalties less effective in driving the deployment rates.

In the case of higher uncertainty allowing bidders to adjust their bids according to different states of the world enhances deployment. If we allow firms to index their bids to solar panel prices, we can allow the firms to adjust tariffs to uncertainty.

---

[7]Battigalli and Maggi (2002) also find that whether to have more contingent clauses or more rigid clauses depends on the level of uncertainty
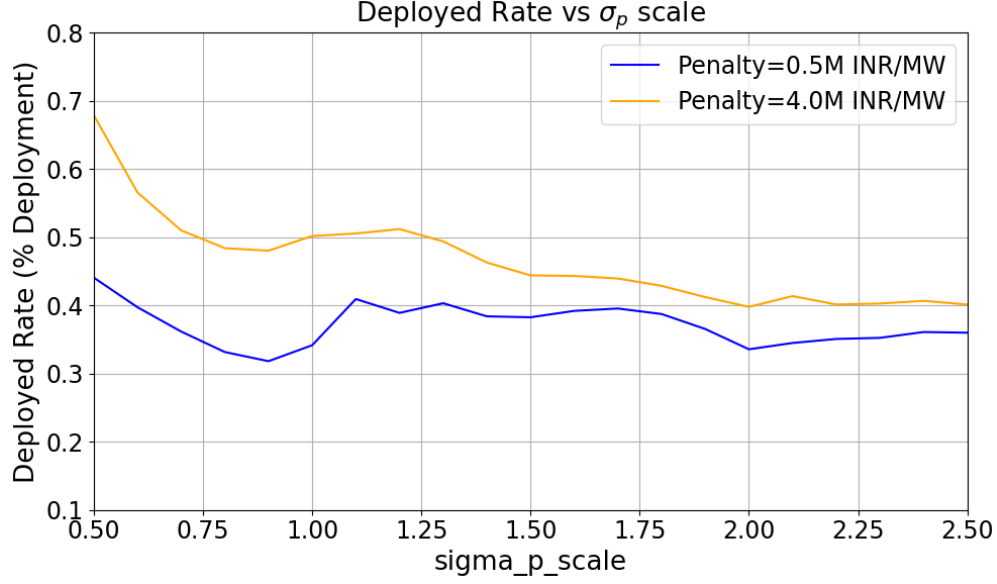
Figure 11: Deployed Capacity vs σ_p scale. The volatility of the stochastic prices process or the σ_p used in the simulation for the iterations is the product of estimated σ_p and corresponding value on the x-axis. For reference of penalty values as compared to benchmark costs, 0.5M INR/MW is in the range of $0.7\% - 1\%$ and 4M INR/MW is in the range of $5.6\% - 8\%$ of average cost per MW (MNRE (2021))

In Figure 12, we observe that increasing the bid index is more effective in boosting the deployment compared to imposing the penalties. Another important observation is the difference in the standard error bands as they are much broader when the penalties are imposed, indicating that the deployment is highly dependent on the price realizations in this scenario. In contrast, when the bids are indexed, the error bands are much narrower, as firms can update their bids based on the different price realizations. However, the bid indexing is expensive and results in increased procurement costs. In the next section, I will discuss how the deployment timings affect the procurement costs in the case of bid indexing.

8.2 Contract design to balance benefits of waiting and deployment

In each period, the firms optimally decide whether to build the project or wait for the next period to learn new information about the costs. Hence, the firm's decision to deploy in each period is naturally modeled based on the value from deployment and the expected value added from waiting conditional on not deploying in that period. This is defined as the

quasi-option value, as, introduced by (Arrow and Fisher (1974)) due to the irreversibility of investments and the net benefit from deployment being dependent on expected benefits from waiting. This has an effect similar to "risk aversion" as there is a reduction in the net benefits from deployment due to the benefits of waiting.
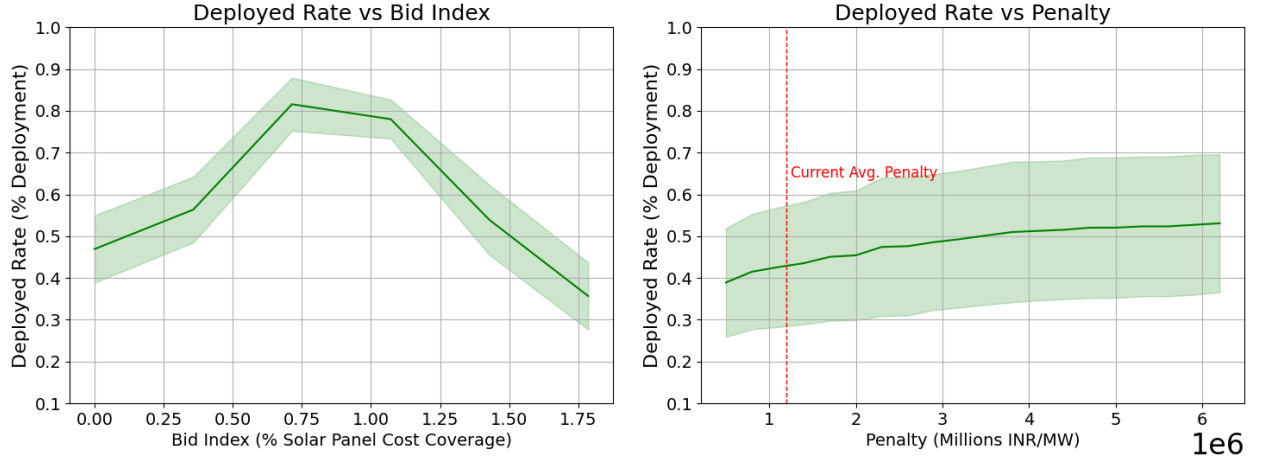
Figure 12: The curves show the mean and standard errors of deployment rates for the counterfactual simulations for 2 cases for the highly volatile case. (i) (left) varying bid index (γ), (ii) (right) varying penalties, for the draws of bidder types and solar panel prices

Even under risk neutrality, the firms behave similarly to the risk-averse firms due to the net benefits of deployment being reduced by the benefits of waiting. This is to say that there are states of the world where the firm would have chosen to build the project had there been certainty but due to uncertainty chose to wait. " This can be interpreted as, if they are uncertain about the payoff to investment in development, they will err on the side of under-investment, rather than over-investment, since development is irreversible " (Arrow and Fisher (1974)). This is true for the baseline case where the firms waited too long and were not able to deploy the projects after the positive input cost shocks. In contrast, bid indexing helps incentivize the firms to invest and assuage the under-investment problem, but it comes at the cost of higher final tariffs.
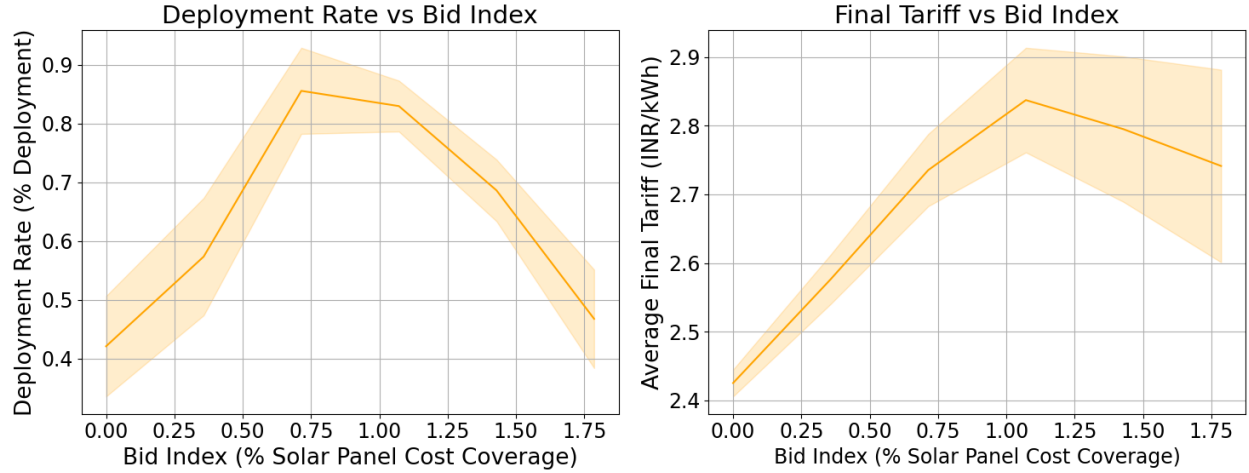
Figure 13: Deployed capacity and Bid prices with increasing bid index. The graph shows how the deployment rate (left) and Average Final Tariff (right) as the bid index parameter (γ) is varied.

Allowing the firms to index their bids to the solar panel prices reduces the incentives for the firms to wait while making the deployment decisions. That is, the increased deployment comes with the trade-off of increasing final tariffs and, consequently, the procurement costs (Figure 13). In certain ranges of the bid indices, deployment does not rise, but tariffs do. This occurs because, when bid indices are high, firms have less incentive to wait for lower prices and end up deploying early, as shown in Figure **??**.

Figure 14 shows how the firms wait less to deploy the projects as the bid index increases, which leads to over-investment at higher prices instead of firms waiting for lower prices. Designing the contracts as incentive contracts can incentivize firms to wait optimally and make the optimal deployment decisions.

The incentive contracts bound the benefits of waiting as the government allows the firms to adjust bids for a proportion of cost overruns and cost under-runs. The bid adjustment parameters should be optimally chosen so that firms do not wait too much (lessen the probability of deployment) or wait too little (raise the costs of deployment).
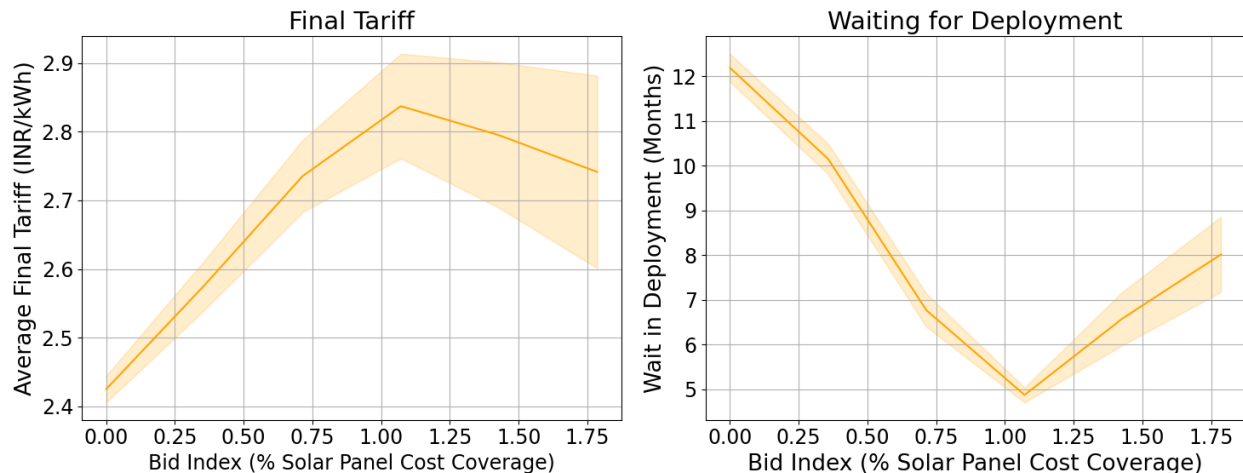
Figure 14: The graph shows how the average final tariff (left) and waiting after the deadline (right) changes as the bid index parameter (γ) is varied. Waiting after the deadline is the number of months from the deadline, the project is deployed and represents how much the firms are waiting to see better solar panel prices instead of deploying in a specific period.

In Figure 15, we see that for the lower range of P_u there is almost the same deployment for both values of $\kappa \in \{60\%, 100\%\}$, with a lower value of κ having the lower final tariffs but higher bids. This occurs because the firms wait longer to realize the lower prices and then deploy the projects when the κ is lower. Whereas for the higher values of P_u, the deployment is higher in the higher κ cases as firms in most future realizations are not allowed to index their bids, and hence, bids in higher κ increase steeply. Also, in the case that the solar panel prices do increase a lot they are allowed to fully index their bid to the cost overrun as κ is 100% which leads to higher deployment.

Consequently, using incentive contracts, firms can be encouraged to wait optimally without significantly reducing the deployment and keeping tariffs relatively constant, compared to allowing firms to adjust their tariffs irrespective of whether price realizations are above or below a threshold.

8.3 Comparative Statics of incentive contract parameters

In this section, I will discuss the comparative statics for different contract parameters to understand how these parameters affect the expected procurement costs and deployment

rates. Additionally, I will explore how the optimal bids and deployment behavior of firms are influenced by these contract parameters.
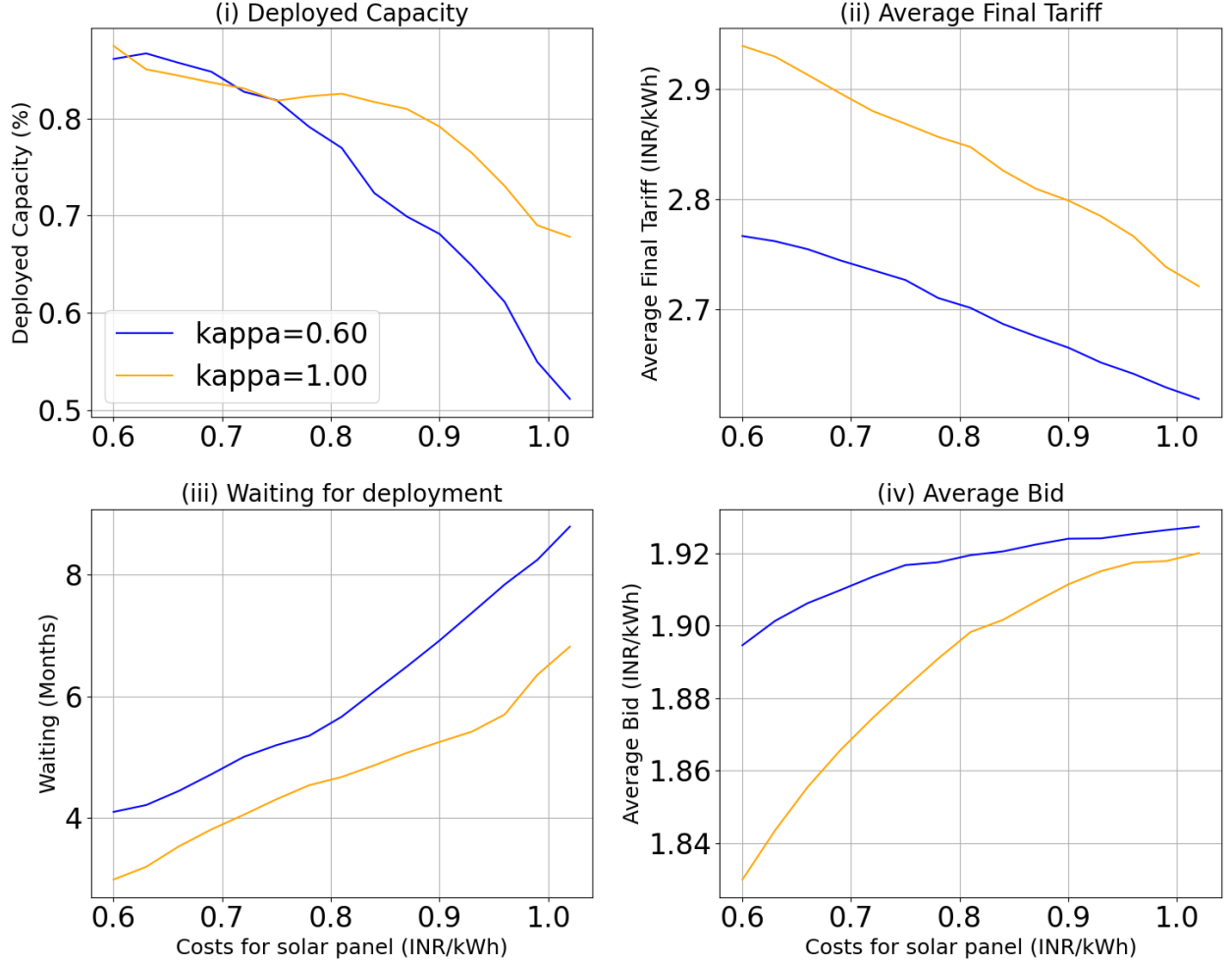

Figure 15: Assuming $P_l = 0.3$ INR/kWh. The results are from simulations for $\kappa \in \{60\%, 100\%\}$ across values of P_u.

Figure 16 shows the effect of the bid indexing parameter (κ) and the price threshold (P_u) for cost overruns. As discussed in the previous section, setting the bid indexing parameter too high or the upper price threshold for cost overruns too low reduces the incentive for firms to wait for better solar panel prices, thereby increasing procurement costs. In the top right 3×1 grid, we observe that the deployment rate is not increasing significantly but procurement costs are rising significantly. This occurs because firms are bidding more initially in the auctions, which keeps the probability of deployment relatively stable. Subsequently, with

a lower bid indexing parameter, firms tend to wait longer to deploy projects, thus keeping procurement costs lower.
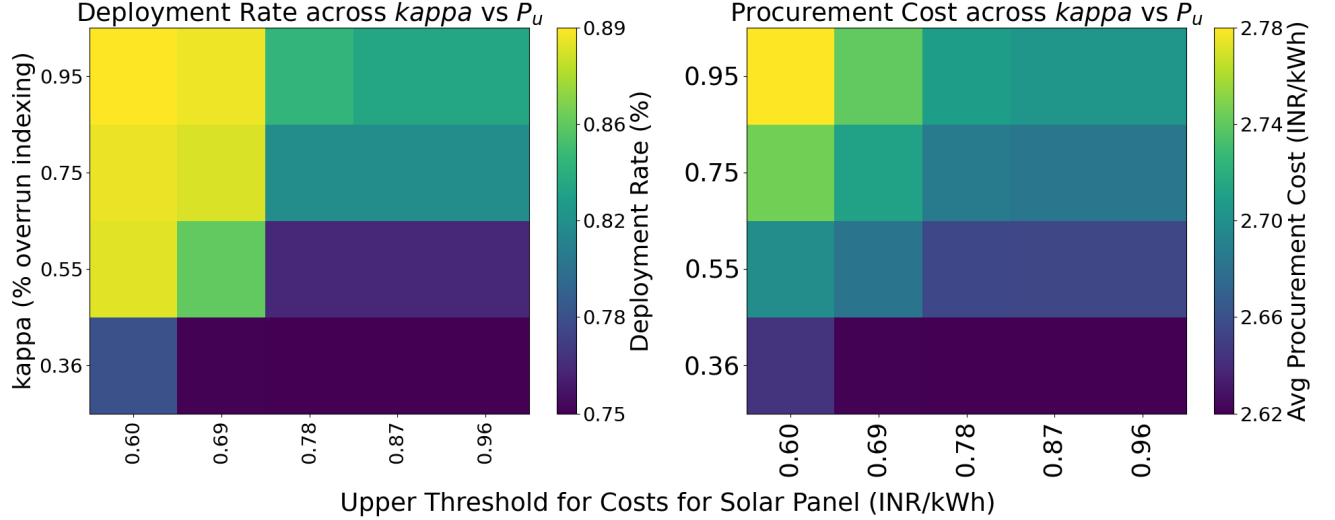
Figure 16: The heat maps show the values of tariffs and deployment rates across the grids of κ and P_u.

The government must set the parameters in a way that incentivizes firms to invest optimally. In doing so, the government makes an optimal trade-off between achieving green energy goals and minimizing procurement costs.

9   Conclusion

The problem addressed in this paper revolves around incomplete contracts in renewable energy procurement auctions, particularly in the Indian solar energy sector. Incomplete contracts that do not account for future uncertainties, such as fluctuating input costs, result in significant non-deployment of solar energy projects. This presents a serious challenge for meeting global renewable energy targets, such as the need for 1000 GW of renewable power annually to achieve net-zero emissions by 2050. In the case of India, only 8 GW of the 22 GW procured through auctions by 2022 had been deployed, largely due to the increase in solar panel costs after 2020. The mismatch between contract terms and changing cost conditions discourages firms from following through on their deployment commitments, underscoring

the need for better contract design in the face of uncertainty.

To address this, I propose an alternative contract design that incorporates two key mechanisms: bid indexing and penalties. Bid indexing allows firms to adjust their bids according to future cost fluctuations, while penalties discourage non-deployment by making it costlier for firms to delay or abandon projects. I develop an incentive contract that combines a fixed component with selective bid indexing and penalties. Through empirical analysis using auction and deployment data from Indian solar procurement auctions, I show that this incentive contract improves deployment rates while keeping tariff increases minimal. Specifically, the incentive contract achieves an 80% increase in deployment with only a 4% rise in tariffs compared to baseline contract designs, outperforming both unconditional bid indexing and penalty-based contracts. The results highlight that selectively allowing bid indexing in response to cost overruns, combined with optimal penalties, can significantly enhance project deployment without imposing excessive costs.

These findings have broader implications for renewable energy procurement and contract design. The results demonstrate that flexible contract mechanisms that account for future uncertainties can align firms' incentives with policy goals, helping governments meet ambitious renewable energy targets while minimizing costs. The suggestion of using incentive contracts to adjust tariffs based on cost overruns and under-runs offers a practical approach to incentivize timely project deployment while managing procurement costs. Other energy auctions, such as the thermal auctions discussed in Ryan (2020), which allow for unconditional bid indexing to the price of coal might result in high tariffs due to the inefficient procurement of coal by the firms. The incentive contracts might help the governments design the contracts such that the firms procure coal optimally and reduce the final tariffs.

The approach used in this paper could be applied to other sectors where investment under uncertainty is a concern, suggesting that incomplete contracts with rigid terms are not well-suited to environments with high-cost volatility. Overall, the paper contributes to the literature on contract theory and procurement auctions by offering a solution to the hold-up problem in green energy transitions, emphasizing the importance of incorporating

future contingencies in procurement mechanisms.

A   Appendix

A.1   Auction Mechanism: Example

This section illustrates the auction process with an example of a solar power procurement auction.

A.1.1   Step 1: Technical Bid Evaluation

SECI examines all documents submitted by the bidders to ensure eligibility based on the RfS criteria. Once all techno-commercial eligibility criteria are met, the evaluation proceeds.

A.1.2   Step 2: Financial Bid Evaluation

In this step, SECI evaluates the tariffs quoted by the bidders in INR/kWh. If multiple bidders submit the same tariff, they are considered equal rank and will all proceed to the reverse auction. Table 2 is an example of the ranking based on the financial bid evaluation, shown in :

Bidder	Submitted Financial Bid (INR/kWh)	Ranking
B1	2.10	L1
B2	2.20	L2
B3	2.30	L3
B4	2.30	L3
B5	2.65	L4
B6	2.70	L5
B7	2.80	L6
B8	2.88	L7
B9	2.88	L7

Table 2: Financial Bid Evaluation and Ranking

A.1.3 Step 3: Reverse Auction

Reverse auctions are conducted electronically, where bidders can submit revised tariffs, decreasing the initial bids by at least 0.01 INR/kWh. During the reverse auction, bidders fall into different zones based on their likelihood of being allocated capacity:

- **Green Zone:** Bidders who may be allocated their full project capacity.

- **Yellow Zone:** Bidders who may receive partial allocation.

- **Red Zone:** Bidders who will not be awarded capacity.

At the end of the reverse auction, the successful bidders are selected based on the lowest discovered tariffs, subject to the available capacity. This is illustrated in Table 3:

Rank	Quoted Capacity (MW)	Cumulative Capacity (MW)	Tariff (INR/kWh)
L1	100	100	2.50
L2	200	300	2.52
L2	400	700	2.52
L3	300	1000	2.54
L4	600	1600	2.55
L5	300	1900	2.55
L5	100	2000	2.55
L5	300	2300	2.56
L6	200	2500	2.70
L7	300	2800	2.90

Table 3: Example of Reverse Auction and Ranking with Color-Coded Tariffs

A.1.4 Selection of Successful Bidders

The total eligible bidders for the reverse auction are decided as follows:

Let: - T = Total number of techno-commercially qualified bidders. - S_k = Cumulative capacity till the 'k'th serial number bidder after ranking is done in ascending order from L1 onwards.

Now, we consider two cases based on the total bid capacity:

- **Case 1:** If $S_T < 1200$ MW, the eligible capacity $S_E = 0.8 \times S_T$.

- **Case 2:** If $S_T \geq 1200$ MW, the eligible capacity $S_E = 0.8 \times S_T$, subject to a maximum of 1200 MW.

For example, consider the shortlisting of bidders for the reverse auction. Let $S_T = 1750$ MW. The shortlisted bidders are calculated as follows:

- If $0.8 \times S_T \leq 1200$ MW, all techno-commercially qualified bidders will be shortlisted for the reverse auction.

- If $0.8 \times S_T > 1200$ MW, the highest-ranked bidder (H1) will be eliminated.

Refer to the tables for examples of financial bid evaluation and reverse auction procedures.

A.2 Value Function

To define the maximization problem, we introduce the value function approach. For any period t, when τ periods are remaining, let $EV^\tau(b, q; c_0, P_t)$ denote the ex-ante value function at the beginning of the period. It is the discounted sum of current and future payoffs just before P_{t+1}, ν_{t+1} are realized and before the decision is made.

Conditional value function for choice d net of ν_{it} and behaving optimally in future:

$$
v_d^\tau(b, q; c_0, P_t) = \begin{cases} \mathbb{E}_{P,\nu|P_t} V^{\tau-1}(b, q; c_0, P_{t+1}) & d = 0 \\ bq - c(c_0, P_t)q & d = 1 \end{cases}
$$

For period, $\bar{T}$, or $\tau = 1$ period remaining,

$$
v_d^1(b, q; c_0, P_{\bar{T}}) = \begin{cases} -Pen & d = 0 \\ bq - c(c_0, P_{\bar{T}})q & d = 1 \end{cases}
$$

Under the assumption that ν_t follows i.i.d Type 1 extreme value distribution, the conditional choice probability is given by,

$$p_1^1(b, q; c_0, P_{\bar{T}}) = \frac{1}{1 + exp[v_0^1(b, q; c_0, P_{\bar{T}}) - v_1^1(b, q; c_0, P_{\bar{T}})]} \tag{16}$$

Given that stochastic price process is given by $\mathcal{J}$, using Rust (1987), expected value function at $\bar{T} - 1$

$$\mathbb{E}_{\nu, P|P_{\bar{T}-1}} V^1(b, q; c_0, P_{\bar{T}}) = \int_{-\infty}^{\infty} \Bigg[ln(exp(v_0^1(b, q; c_0, P_{\bar{T}})) +$$

$$exp(v_1^1(b, q; c_0, P_{\bar{T}}))) \Bigg] j(P_{\bar{T}}|P_{\bar{T}-1}) dP_{\bar{T}}$$

For finding the Bayesian Nash Equilibrium, given the Information Set $\mathcal{I}_0 = \{P_0, c_0\}$. Hence, using iterated expectations

$$\mathbb{E}_{\nu, P|P_0}[\mathbb{E}_{\nu, P|P_{\bar{T}-1}} V^1(b, q; c_0, P_{\bar{T}})] = \mathbb{E}_{\nu, P|P_0} V^1(b, q; c_0, P_{\bar{T}})$$

Solving for BNE would require, forming beliefs on the state of the world on the basis of the current information set. Hence at $t = 0$,

$$\mathbb{E}_{\nu, P|P_0} V^1(b, q; c_0, P_{\bar{T}}) = \int_{-\infty}^{\infty} \Bigg[ln(exp(v_0^1(b, q; c_0, P_{\bar{T}})) +$$

$$exp(v_1^1(b, q; c_0, P_{\bar{T}}))) \Bigg] j(P_{\bar{T}}|P_0) dP_{\bar{T}}$$

A.3 Isotone Perfect Strategy equilibrium

Assumption 3 *Each player $i = 1, \ldots, n$ has a common action set $L \in \mathbb{R}^k$ that is a finite sublattice of k-dimensional Euclidean space with respect to the product order on $\mathbb{R}^k$.*

Assumption 4 *Player i's type t_i is drawn from common support $T = [0,1]^h$. The joint density on type profiles (or states) $t = (t_1, \ldots, t_n)$, $f : \mathbb{R}^{nh} \to \mathbb{R}_{++}$, is bounded above by $\bar{K}$ and bounded below by $\underline{K} > 0$. The type space is endowed with the product order and the usual Euclidean topology and measure.*

Assumption 5 *Ex-post payoff is bounded and measurable.*

Assumption 6 *Interim expected payoff is quasi-supermodular in a_i for all $t_i \in T$ and all $a_{-i}(.) \in \mathcal{J}_{-i}$.*

Assumption 7 *Interim expected payoff satisfies the single crossing property in (a_i, t_i) for all $a_{-i}(.) \in \mathcal{J}_{-i}$.*

Sufficient Primitive Conditions for Assumptions 4 and 5 (McAdams (2003) and Topkis (1979)):

Types are independent and ex-post payoff is supermodular in a_i with non-decreasing differences in (a_i, t_i). Then expected interim-payoff is supermodular in a_i and has nondecreasing differences in (a_i, t_i) when $a_{-i}(.) \in \mathcal{J}_{-i}$. (Others may follow any strategies.)

Assumption 8 *$EV(.)$ satisfies non-decreasing differences in (b_i, t_i), where $t_i = (c_{i0}, q_i)$ is the bidder type.*

Discussion on uniqueness of equilibrium

A.4 Results and functional assumptions

I make the following functional assumptions to estimate the stochastic price process and bidder types:

- **Stochastic Price Process**: $GBM(\mu_p, \sigma_p)$

- **Bidder type**: $(c_0, q) \sim log - N(\mu, \Sigma)$, where μ is

$$\begin{pmatrix} \mu_{c_0} \\ \mu_q \end{pmatrix}$$

and Σ is

$$\begin{pmatrix} var_{c_0} & cov_{c_0q} \\ cov_{c_0q} & var_q \end{pmatrix}$$

and Table 4 shows the estimated model parameters:

Parameter	Description	Value (Standard Error)
Cost Distribution Parameters		
μ_{c_0}	Mean of log of private cost signal	0.39 (0.07)
μ_q	Mean of of log of capacity	5.70 (1.8)
σ_{c_0}	Standard deviation of log private cost signal	0.35 (0.08)
σ_q	Standard deviation of log capacity	5.54 (0.52)
cov_{c_0q}	Covariance of log of private cost signal and capacity	-1.37 (0.4)
β	Price coefficient	2.8 (0.5)
Stochastic Price Process Parameters		
μ_P	Mean of price process	-0.06 (0.03)
σ_P	Standard deviation of price process	0.27 (0.11)
Scale Parameter		
$1/\sigma$	Scale parameter of idiosyncratic shocks	0.7 (0.2)

Table 4: Estimated Model Parameters

A.5 Effect of price volatility on break-even bids: Illustrative

As shown in Figure 17, in more volatile cases, prices are higher in bad states and lower in good states compared to the less volatile case. As the firms can wait to realize good states and choose not to deploy in the bad states, their break-even bids decrease as the price volatility increases (Figure 18).
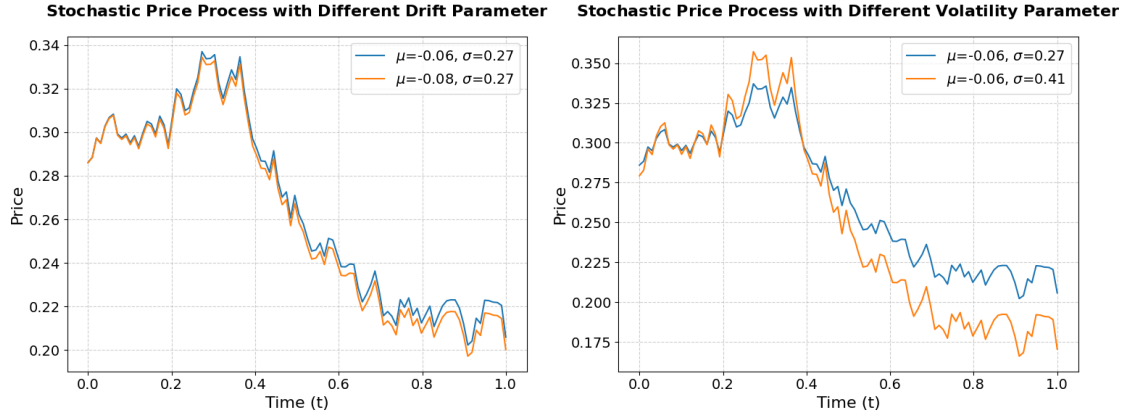
Figure 17: Stochastic Price Process in different μ_p and σ_p
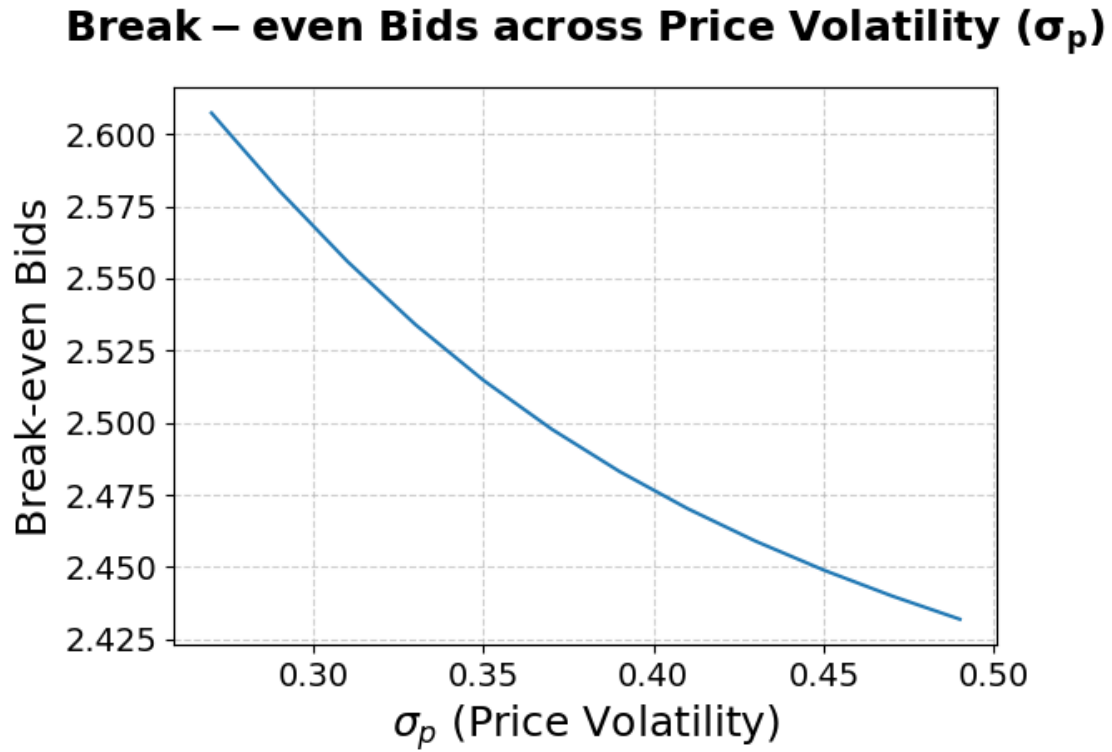

Figure 18: Illustrative: Break-even bid for $q = 250$, $c_0 = 0.7$

References

Arcidiacono, P. and R. A. Miller (2011). Conditional choice probability estimation of dynamic discrete choice models with unobserved heterogeneity. *Econometrica 79*(6), 1823–1867.

Arrow, K. J. and A. C. Fisher (1974). Environmental preservation, uncertainty, and irreversibility. *The Quarterly Journal of Economics 88*(2), 312–319.

Battigalli, P. and G. Maggi (2002, September). Rigidity, discretion, and the costs of writing contracts. *American Economic Review 92*(4), 798–817.

Bhattacharya, V., A. Ordin, and J. W. Roberts (2022, May). Bidding and drilling under uncertainty: An empirical analysis of contingent payment auctions. *Journal of Political Economy 130*(5).

DeMarzo, P. M., I. Kremer, and A. Skrzypacz (2005). Bidding with securities: Auctions and security design. *American economic review 95*(4), 936–959.

Dempster, A. P., N. M. Laird, and D. B. Rubin (1977). Maximum likelihood from incomplete data via the em algorithm. *Journal of the royal statistical society: series B (methodological) 39*(1), 1–22.

Donald, S. G. and H. J. Paarsch (1996, July). Identification, estimation, and testing in parametric empirical models of auctions within the independent private values paradigm. *Econometric Theory 12*(12), 517–67.

Grossman, S. J. and O. D. Hart (1986). The costs and benefits of ownership: A theory of vertical and lateral integration. *Journal of political economy 94*(4), 691–719.

Hart, O. and J. Moore (1988). Incomplete contracts and renegotiation. *Econometrica 56*, 755–785. Accessed 22 July 2024.

Herrnstadt, E., R. Kellogg, and E. Lewis (2024). Drilling deadlines and oil and gas development. *Econometrica 92*(1), 29–60.

Hotz, V. J. and R. A. Miller (1993). Conditional choice probabilities and the estimation of dynamic models. *The Review of Economic Studies 60*(3), 497–529.

IRENA (2023). World energy transitions outlook 2023. Accessed: 2023-07-15.

Joskow, P. L. (1987). Contract duration and relationship-specific investments: Empirical evidence from coal markets. *The American Economic Review*, 168–185.

Klein, B., R. G. Crawford, and A. A. Alchian (1978). Vertical integration, appropriable rents, and the competitive contracting process. *The journal of Law and Economics 21*(2), 297–326.

Kong, Y., I. Perrigne, and Q. Vuong (2022, May). Multidimensional auctions of contracts: An empirical analysis. *American Economic Review 112*(5), 1703–36.

Laffont, J.-J. and J. Tirole (1986). Using cost observation to regulate firms. *Journal of political Economy 94*(3, Part 1), 614–641.

Laffont, J.-J. and J. Tirole (1987). Auctioning incentive contracts. *Journal of Political Economy 95*(5), 921–937.

Lewis, G. and P. Bajari (2011). Procurement contracting with time incentives: Theory and evidence. *The Quarterly Journal of Economics 126*(3), 1173–1211.

McAdams, D. (2003, July). Isotone equilibrium in games of incomplete information. *Econometrica 71*(4), 1191–214.

McAfee, R. P. and J. McMillan (1986). Bidding for contracts: a principal-agent analysis. *The RAND Journal of Economics*, 326–338.

Milgrom, P. R. and R. J. Weber (1982, July). A theory of auctions and competitive bidding. *Econometrica 50*(5), 1089–122.

Nunn, N. (2007). Relationship-specificity, incomplete contracts, and the pattern of trade. *The quarterly journal of economics 122*(2), 569–600.

Ryan, N. (2020). Contract enforcement and productive efficiency: Evidence from the bidding and renegotiation of power contracts in india. *Econometrica 88*(2), 383–424.

Ryan, N. (2021). Holding up green energy. Technical report, National Bureau of Economic Research.

Tirole, J. (1999). Incomplete contracts: Where do we stand? *Econometrica 67*(4), 741–781.

Topkis, D. M. (1979). Equilibrium points in nonzero-sum n-person submodular games. *Siam Journal on control and optimization 17*(6), 773–787.